OPEN ACCESS Freely available online

PLoS GENETICS

# The *Caenorhabditis elegans* Mucin-Like Protein OSM-8 Negatively Regulates Osmosensitive Physiology Via the Transmembrane Protein PTR-23

**Anne-Katrin Rohlfing[¤a], Yana Miteva[¤b], Lorenza Moronetti, Liping He, Todd Lamitina***

Department of Physiology, University of Pennsylvania, Philadelphia, Pennsylvania, United States of America

## Abstract

The molecular mechanisms of animal cell osmoregulation are poorly understood. Genetic studies of osmoregulation in yeast have identified mucin-like proteins as critical regulators of osmosensitive signaling and gene expression. Whether mucins play similar roles in higher organisms is not known. Here, we show that mutations in the *Caenorhabditis elegans* mucin-like gene *osm-8* specifically disrupt osmoregulatory physiological processes. In *osm-8* mutants, normal physiological responses to hypertonic stress, such as the accumulation of organic osmolytes and activation of osmoresponsive gene expression, are constitutively activated. As a result, *osm-8* mutants exhibit resistance to normally lethal levels of hypertonic stress and have an osmotic stress resistance (Osr) phenotype. To identify genes required for Osm-8 phenotypes, we performed a genome-wide RNAi *osm-8* suppressor screen. After screening ~18,000 gene knockdowns, we identified 27 suppressors that specifically affect the constitutive osmosensitive gene expression and Osr phenotypes of *osm-8* mutants. We found that one suppressor, the transmembrane protein PTR-23, is co-expressed with *osm-8* in the hypodermis and strongly suppresses several Osm-8 phenotypes, including the transcriptional activation of many osmosensitive mRNAs, constitutive glycerol accumulation, and osmotic stress resistance. Our studies are the first to show that an extracellular mucin-like protein plays an important role in animal osmoregulation in a manner that requires the activity of a novel transmembrane protein. Given that mucins and transmembrane proteins play similar roles in yeast osmoregulation, our findings suggest a possible evolutionarily conserved role for the mucin-plasma membrane interface in eukaryotic osmoregulation.

**Citation:** Rohlfing A-K, Miteva Y, Moronetti L, He L, Lamitina T (2011) The *Caenorhabditis elegans* Mucin-Like Protein OSM-8 Negatively Regulates Osmosensitive Physiology Via the Transmembrane Protein PTR-23. PLoS Genet 7(1): e1001267. doi:10.1371/journal.pgen.1001267

**Editor:** Miriam B. Goodman, Stanford University School of Medicine, United States of America

**Received** April 9, 2010; **Accepted** December 3, 2010; **Published** January 6, 2011



**Funding:** This research was supported by NIH NIAAA/NIEHS 1R01AA017580 to TL. Some nematode strains used in this work were provided by the Caenorhabditis Genetics Center, which is funded by the NIH National Center for Research Resources (NCRR). The funders had no role in study design, data collection and analysis, decision to publish, or preparation of the manuscript.

**Competing Interests:** The authors have declared that no competing interests exist.

* E-mail: lamitina@mail.med.upenn.edu

¤a Current address: Institut für Biochemie und Biologie, Universität Potsdam, Golm, Germany
¤b Current address: Graduate Program in Molecular Biology, Princeton University, Princeton, New Jersey, United States of America

## Introduction

Cell volume is one of the most aggressively defended homeostatic set points in biology. In response to alterations in tonicity, virtually all cells activate mechanisms to regulate cell water and solute content [1]. To counteract decreases in cell volume caused by hypertonic conditions, cells restore volume through the rapid accumulation of ions and water via the activation of various plasma membrane ion conductance pathways [2]. Increased ion accumulation raises cytoplasmic ionic strength, which can disrupt protein structure and function [3]. Cytoplasmic ionic strength is lowered by the relatively slow accumulation of organic osmolytes (ie. glycerol, sorbitol, myo-inositol, etc), which are non-ionic solutes that can be accumulated to high (100s of mM) concentrations without affecting cell structure and/or protein function [4]. Organic osmolytes accumulation is mediated by metabolic biosynthesis or transport into the cell via specialized organic osmolyte transporter proteins [5]. In virtually all cells, the biosynthesis and/or transporters that mediate organic osmolyte accumulation are transcriptionally upregulated by hypertonicity [6,7,8,9].

While the effector molecules that mediate ion, water, and osmolyte accumulation are generally well understood, the molecular mechanisms that allow cells to sense changes in cell volume and activate appropriate solute accumulation pathways are poorly defined. Molecular mechanisms of osmosensing are best understood in unicellular organisms, such the yeast *S. cerevisae*, where elegant genetic studies have identified specialized MAPK signaling pathways which direct osmosensitive gene expression [10]. While MAPKs are highly conserved from yeast to humans, animal genomes do not contain homologs of upstream molecules that are thought to sense changes in cell volume and activate MAPK signaling, such as the transmembrane proteins Sln1 and Sho1. The absence of these proteins has lead to speculation that animals utilize different molecular mechanisms for sensing osmotic challenges. Several such alternative mechanisms have been proposed, including detection of membrane tension, mechanical 'stretch', macromolecular crowding [11], and detection of osmotically-induced protein damage [12]. However, molecular data on the nature of such an 'osmosensor' in animal cells has not been forthcoming.

## Author Summary

The ability to sense and respond to changes in cell volume is a process termed osmoregulation and is an essential prerequisite for cellular life. While the molecular details of this physiological process are well described in unicellular organisms such as yeast and bacteria, the mechanisms that govern osmoregulation in animals are poorly understood. Using a genetic approach in the nematode *C. elegans*, we identified the mucin-like protein OSM-8 as a critical regulator of osmoregulation. Disruption of the *osm-8* gene results in the activation of physiological responses that are normally only activated in response to hyperosmotic stress, suggesting that *osm-8* is a negative regulator of *C. elegans* osmoregulatory physiology. Through a genome-wide RNAi suppressor screen, we also identified a transmembrane protein, PTR-23, that is required for *osm-8* mutants to activate osmoregulatory physiological responses. Together with previous findings from yeast, our data define an important and possibly evolutionarily conserved role for the plasma membrane-mucin matrix interface in eukaryotic osmoregulation. Our findings also illustrate the value of studying cell physiological processes such as osmoregulation in a live animal model, in which complex and dynamic extracellular matrix structures are preserved.


Mucins are a class of secreted glycoprotein that are produced by almost all non-keratinized epithelial cells [13]. Mucins are broadly defined by the presence of repeated domains rich in proline, serine, and/or threonine and can either be secreted or remain tethered to the plasma membrane via a transmembrane (TM) domain. Secreted and TM mucins play a barrier role in epithelia, protecting against both pathogen attack and environmental toxins. Secreted mucins can form gel-like matrices (the so-called 'gel-forming' mucins) that can shrink and swell in response to environmental solute and water levels [13,14]. Mucins can also participate in the regulation of cellular signaling pathways, both through their cytoplasmic regions (in the case of TM mucins) and through interactions with other ECM molecules. Outside their function as barrier molecules, the physiological roles of mucins in animals are poorly understood. Recent studies in yeast have revealed that mucins play key roles in the regulation of the MAP kinase signal transduction pathway that controls osmosensitive gene expression and organic osmolyte (glycerol) accumulation [15]. A role for mucins in animal osmotic stress responses has been postulated [16], but evidence to support this hypothesis is lacking.

The nematode *C. elegans* has emerged as a genetic model system for the analysis of animal osmotic stress responses [8,12,17,18,19]. Similar to yeast, hypertonic stress in *C. elegans* activates rapid accumulation of the organic osmolyte glycerol via de novo biosynthesis. Glycerol biosynthesis is preceded by the rapid transcriptional upregulation of the glycerol-3-phosphate dehydrogenate enzyme *gpdh-1* in the intestine and hypodermis, two epithelial tissues that are in direct contact with the environment. Activation of *gpdh-1* expression is highly specific and is not activated by any stressor other than hypertonicity [12]. Induction of *gpdh-1* expression by osmotic stress does not depend on other known stress response signaling pathways, including the *daf-2/daf-16* insulin-like pathway or the *pmk-1*-dependent MAP kinase pathway [17,20]. These studies suggest that the activation of osmosensitive gene expression in *C. elegans* utilizes novel signaling mechanism(s) and that detailed analysis of this pathway may shed new light on the molecular nature of osmosensing in animals.

Recently, both forward and reverse genetic approaches have identified negative regulators of *gpdh-1* expression that result in robust activation of osmosensitive gene expression in the absence of hypertonic stress [12,18,19,21]. Among these genes were two osmotic avoidance defective (*osm*) genes, *osm-7* and *osm-11*, that were previously identified in behavioral screens for mutants that fail to avoid hyperosmotic stimuli [18]. Here, we show that another Osm gene, *osm-8*, is also a negative regulator of whole-animal osmotic stress response mechanisms in *C. elegans*. We cloned *osm-8* and found that it encodes a mucin-like protein. OSM-8 functions as a secreted protein in the cuticle extracellular matrix to regulate both hypodermal and intestinal *gpdh-1* expression. *osm-8* is not required for overall cuticle organization or function, nor is it required for development of the underlying epidermis, suggesting that *osm-8* plays a specific role in osmoregulatory physiology. By performing a genome-wide RNAi screen for *osm-8* suppressors and enhancers, we discovered that *osm-8* phenotypes are dependent on the gene *ptr-23*, which encodes a predicted plasma membrane localized multipass transmembrane domain protein that is co-expressed with *osm-8* in the hypodermis. Our identification of a mucin-like protein and a downstream transmembrane protein as regulators of osmosensitive gene expression in *C. elegans* is remarkably similar to studies of osmoregulation in yeast and supports a role for mucins as evolutionarily conserved regulators of cellular osmosensing.

## Results

### *osm-8* mutants inappropriately activate *gpdh-1* expression and glycerol accumulation and are specifically resistant to osmotic stress

Previous genetic screens have identified numerous genes affecting behavioral avoidance of hyperosmotic environments (*osm* genes) [22]. Recently, loss of two Osm genes, *osm-7* and *osm-11*, were shown to mimic whole animal physiological responses to hyperosmotic stress, such as accumulation of glycerol and activation of an osmosensitive transcriptional reporter in the intestine and hypodermis [12,18]. We screened additional Osm genes with a GFP reporter under the control of the glycerol-3-phosphate dehydrogenase 1 promoter (*gpdh-1p::GFP*), a gene whose expression is normally only activated under hyperosmotic conditions. We found that *osm-8(n1518)* mutants activated intestinal and hypodermal *gpdh-1p::GFP* expression in the absence of hypertonicity (Figure 1A). Quantitative analysis of steady state *gpdh-1::GFP* expression revealed that *osm-8(n1518)* mutants caused a 4.4-fold upregulation of the *gpdh-1::GFP* reporter which could be further upregulated following exposure to 200 mM NaCl (Figure 1B), suggesting that *osm-8* mutants retain some ability to detect environmental osmotic alterations. Consistent with the observed upregulation of *gpdh-1*, we also found that *osm-8(n1518)* animals grown under isotonic conditions exhibit ~300-fold elevations in whole worm glycerol levels compared to wild type animals (Figure 1C). As previously shown by microarray analysis [21], *osm-8* animals upregulated the mRNA levels of many osmotically inducible genes in addition to *gpdh-1* (Figure S1), suggesting that *osm-8* mutants activate the osmosensitive gene expression program. *osm-8* mutants did not upregulate other stress-inducible genes, such as the heat shock-inducible genes *hsp-16.2*, *hsp-70*, or the ER stress inducible gene *hsp-4* (Figure S1) and were not significantly resistant to either thermal or oxidative stress (Figure S2). However, *osm-8* mutants were highly resistant to normally lethal levels of hypertonic stress and exhibited an age-dependent osmotic stress resistance (Osr) phenotype (Figure 1D, Video S1). Together, these data suggest that *osm-8* specifically

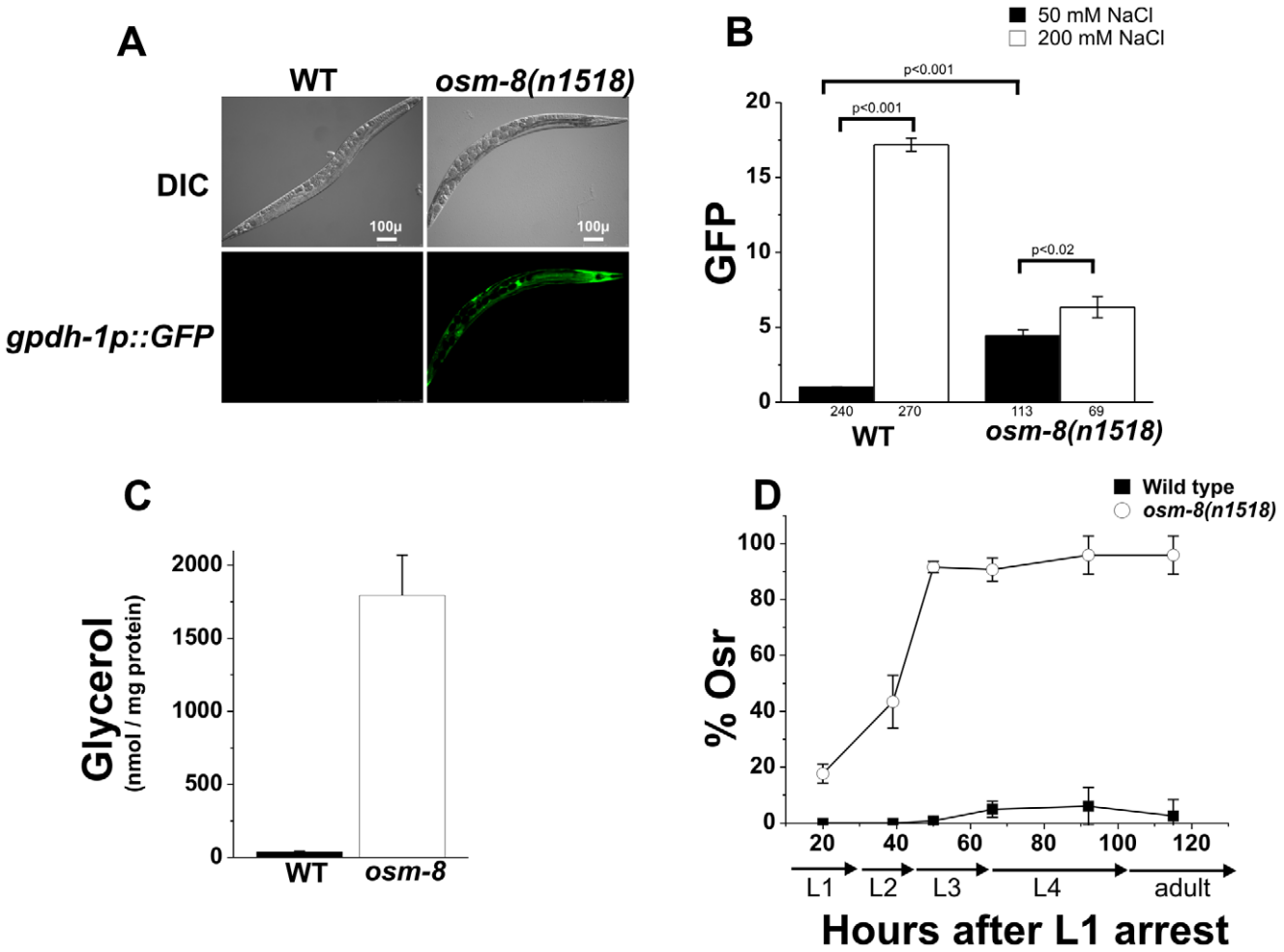


**Figure 1. *osm-8* mutants constitutively activate osmosensitive gene expression and glycerol biosynthesis in the absence of hypertonic stress.** A) DIC and GFP fluorescence images of wild type or *osm-8(n1518)* mutant adults in a *gpdh-1::GFP* transgenic background under standard isotonic (51 mM NGM) culture conditions. Scale bar = 100 µ. B) COPAS quantification of *gpdh-1::GFP* expression in wild type or *osm-8* mutants exposed to either standard NGM (51 mM NaCl, black) or 200 mM NaCl (white) for ~18 h. Data were normalized as described in 'Materials and Methods'. The number of animals sorted for each condition is indicated below each bar graph. C) Glycerol measurements in wild type (black) and *osm-8(n1518)* (white) animals. N = 3 replicates for each genotype. D) Acute osmotic stress resistance phenotype of wild type (black squares) or *osm-8(n1518)* (white circles) as a function of age. The percent of animals still motile after 10 minutes (% Osr) is indicated. For these and all other Osr assays, animals were raised on standard NGM plates (50 mM NaCl) prior to the assay. N>40 animals for each genotype per time point.
doi:10.1371/journal.pgen.1001267.g001

regulates osmotic stress resistance without affecting other stress response mechanisms.

While *osm-8* appeared to specifically affect pathways contributing to osmoregulatory physiology, we considered the possibility that it might function through indirect mechanisms, such as changes in cuticle permeability or epidermal development. To test if *osm-8* alters cuticle permeability, we stained live *osm-8(n1518)* mutant animals with the DNA dye Hoechst 33258. Hoechst dye staining has been previously used to probe the cuticle permeability of various *C. elegans* strains [23,24,25]. Staining in *osm-8(n1518)* animals was identical to wild type animals (Figure S3), suggesting that *osm-8* does not substantially alter cuticle permeability. To test whether cuticle permeability played a role in the Osr phenotype of *osm-8* mutants, we generated *osm-8; bus-8* double mutants. *bus-8* mutants have previously been shown to dramatically increase cuticle permeability [23], and we confirmed that this was also true in the *osm-8(n1518)* background (Figure S3). Despite having increased cuticle permeability, *osm-8; bus-8* double mutants were still Osr (Figure S4), suggesting that alterations in cuticle permeability do not contribute to the Osr phenotype of *osm-8* mutants. Finally, we asked whether an aspect of epidermal development, seam cell fusion, was affected by *osm-8* using an AJM-1-GFP marker [26]. *osm-8* mutant animals exhibited appropriate seam cell development in early larval stages and these cells fused in an appropriate manner later in development (Figure S5). Together, our data demonstrate that *osm-8(n1518)* mutants cause constitutive activation of osmosensitive gene expression and glycerol accumulation and that the activation of osmoregulatory physiological pathways in *osm-8(n1518)* mutants results in the specific resistance to osmotic stress in *C. elegans*. Importantly, our data strongly suggest that Osm-8 phenotypes do not result from alterations in cuticle permeability or in defects in epidermal cell fusion.

## *osm-8* encodes a mucin-like protein

To better understand the mechanisms underlying *osm-8* mediated osmotic stress resistance, we molecularly identified the gene affected by the *osm-8(n1518)* mutation using three different

approaches (Figure 2). First, after mapping *osm-8(n1518)* to a small genetic interval on LGII, we identified a set of overlapping fosmid clones that rescued the *osm-8(n1518)* Osr phenotype (Figure 2A). Of the three predicted ORFs in this overlapping region, we found that a wild type PCR product containing both upstream and downstream sequence for one of these ORFs, R07G3.6, was sufficient to rescue the *osm-8* Osr and *gpdh-1::GFP* overexpression phenotypes (Figure 2C–2E). An identical PCR product derived from the *osm-8(n1518)* background failed to rescue the Osr phenotype (Figure 2D). Second, sequencing of R07G3.6 in *osm-8(n1518)* mutants revealed a G→A mutation that was not present in our wild type strain (Figure 2B). This mutation is predicted to cause a nonsense mutation (W109STOP) in the R07G3.6 coding sequence, just prior to the first Proline/Threonine (PT) repeat domain (see below). Interestingly, animals carrying either of two deletion alleles of R07G3.6, *ok3650* and *tm3693*, were not Osr. Both alleles result in C-terminal truncations that delete either part of PT3 and PT4 (*ok3650* - T169 to G331, leaving the native STOP codon) or a portion of the C-terminus outside of the PT domains (*tm3693* - D213 to Y288 deleted, resulting in early STOP due to frameshift), suggesting that the region between W109 and T169, which contains PT1 and PT2, is critical for OSM-8 function. In support of the functionality of the deletion alleles, we found that a PCR product of the *osm-8* genomic locus derived from the largest deletion allele, *ok3650,* was sufficient to rescue the Osr phenotype of *osm-8(n1518)* mutants (Figure 2D). Finally, we found that RNAi of R07G3.6 in RNAi hypersensitive backgrounds (*rrf-3* and *eri-1*) or over multiple generations of RNAi feeding in wild type animals (data not shown) was sufficient to produce an Osr phenotype identical to that seen in *osm-8(n1518)* mutants (Figure 2C). Together, these three lines of evidence demonstrate that *osm-8* is encoded by R07G3.6.

We cloned the full-length *osm-8* cDNA using 5′RACE and found that it matches the predicted cDNA sequence, suggesting a protein of 330 amino acids. We identified a strong signal sequence motif in the N-terminus of the protein. *osm-8* expression constructs lacking this signal sequence motif were unable to rescue *osm-8(n1518)* Osr phenotypes, suggesting that OSM-8 is a secreted protein (data not shown). The only other recognizable domain in the OSM-8 protein is a proline/serine/threonine rich (PST) domain that is 29.7% identical to a similar domain found in human mucin 2 (Muc2). Muc2 is a large (5179 amino acids) gel-forming mucin that is secreted from most non-keratinized epithelial cells. The central domain of Muc2 is composed of a tandem repeats of PST domains. These sequences are heavily glycoslyated *in vivo* and give the mucin its gel-like properties [13]. While the OSM-8 protein also contains several PST domains within its central region, the domains are not precise repeats and do not contain any serine residues as is characteristic of some, but not all, mucin PST domains (PT domains, Figure 2B). Overall, these data suggest that *osm-8* encodes a secreted protein with features similar to those found in the mucin proteins made and secreted by mammalian epithelial cells.

## *osm-8* is expressed in the hypodermis and expression oscillates through development

Given that *osm-8* encodes a secreted protein, it is likely to act in a cell non-autonomous fashion. To better understand the location(s) from which *osm-8* might be secreted, we determined the sites of *osm-8* expression by constructing transgenic animals expressing an *osm-8p::GFP* transcriptional reporter. This reporter utilized the same promoter that was sufficient for rescue of Osm-8 phenotypes, suggesting it reflects sites of expression necessary for *osm-8* function. In multiple transgenic lines, GFP expression was observed in the hypodermal syncitium and was excluded from the hypodermal seam cells (Figure 3A, 3B). We were unable to visualize the site(s) of OSM-8 protein localization in live L4 or adult animals using an *osm8p::OSM-8-GFP* translational reporter, although animals carrying this translational GFP fusion were fully rescued for *osm-8* mutant phenotypes and fusion protein of the appropriate molecular weight was weakly detected by western blotting using anti-GFP antibodies (data not shown). Such lack of fluorescent signal may be due to improper folding and/or stability of the GFP epitope in the extracellular oxidative milieu or to folding constraints imposed on OSM-8 in its extracellular matrix environment (see below). Transcriptional *osm-8p::GFP* reporter expression was not altered by exposure to hypertonicity or by inhibition of other Osm genes, such as *osm-7* or *osm-11* (data not shown), consistent with previous microarray findings [21]. While the *osm-8* promoter was active in larval stages up to and including the L4, expression in adults was strongly attenuated, suggesting that *osm-8* mRNA expression might be developmentally regulated. Indeed, quantitative RT-PCR analysis of *osm-8* mRNA showed weakly oscillating expression levels that were similar to the expression levels in another secreted protein, the collagen gene *dpy-7* (Figure 3C–3G). Other Osm gene mRNAs either showed no developmental oscillations (*osm-7*) or oscillation patterns that were distinct from *osm-8* (*osm-11*). These data suggest that *osm-8* is robustly expressed during the time of cuticular extracellular matrix synthesis and then strongly downregulated during adulthood and this regulation is distinct from other Osr genes, such as *osm-7* and *osm-11*.

## Overexpression of *osm-8* in the hypodermis rescues Osm-8 phenotypes

Since the OSM-8 protein is expressed and likely secreted from the hypodermis, it could function in either of two locations to regulate osmotic stress responses. First, OSM-8 could be secreted from the basolateral membrane of the hypodermal syncitium to function in the pseudocoelomic space. Alternatively, OSM-8 could be secreted from the apical membrane of the hypoderm to function in the cuticular extracellular matrix space. If OSM-8 is secreted from the basolateral membrane, expression and secretion of OSM-8 from other cells facing this compartment (i.e. intestine, muscle, hypodermis, etc.) should also rescue the Osr phenotypes of *osm-8* mutants. However, if OSM-8 is secreted from the apical membrane to function in the extracellular matrix, then the Osr phenotypes of *osm-8* mutants should only be rescued by expression in ECM-facing tissues (i.e. hypodermis). To distinguish between these possibilities, we generated constructs in which the *osm-8* genomic DNA was under the control of various cell-type specific promoters. *osm-8* expressed under the control of intestine, muscle, or neuronal promoters failed to rescue the Osr phenotype of *osm-8* mutants (Figure 4). However, expression of *osm-8* using the hypodermal specific promoter *dpy-7p* fully rescued the Osr phenotype of *osm-8(n1518)* (Figure 4A). Notably, *dpy-7p::OSM-8* transgenic animals also exhibited hypersensitivity to osmotic stress (Figure 4B, 4C) demonstrating that while loss of *osm-8* function produces osmotic stress resistance, *osm-8* overexpression in the hypodermis produces osmotic stress sensitivity. Taken together, these data suggest that OSM-8 is secreted from the apical membrane of the hypodermis into the extracellular matrix space where its loss causes inappropriate activation of the osmotic stress response in *C. elegans*.

## Acute expression of *osm-8* prior to the L4 molt is sufficient to rescue *osm-8* mutant phenotypes

*osm-8* could contribute to osmoregulatory signaling via multiple mechanisms. For example, *osm-8* could function as an acute

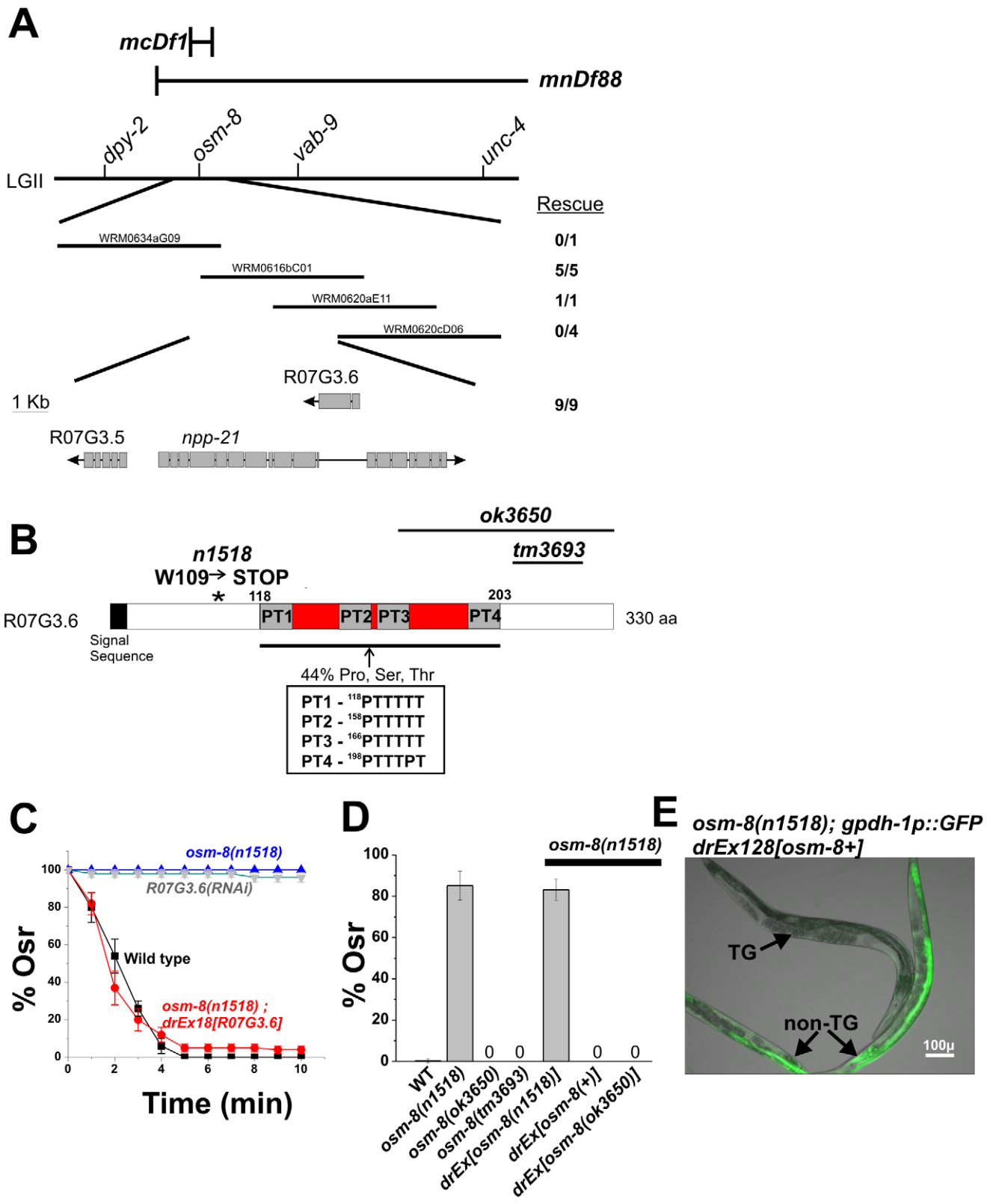


**Figure 2. *osm-8* encodes the mucin-like protein R07G3.6.** A) Genetic mapping of the *osm-8(n1518)* mutation. *n1518* was mapped between *dpy-2* and *vab-9* by multi-factor mapping. Fosmids within this genetic interval are shown. For each fosmid, the number of transgenic lines containing the fosmid that rescued the *osm-8(n1518)* Osr phenotype are shown. Three predicted genes within the overlapping fosmid rescue interval are shown and the number of rescuing transgenic lines from a PCR product of the R07G3.6 gene is indicated. B) Sequence analysis and domain structure of the R07G3.6 gene. The location of the signal sequence and the *n1518* mutation is shown. The inset shows the amino acid sequence of the proline/threonine repeats within the mucin domain. The protein regions removed by the deletion alleles *ok3650* and *tm3693* are indicated by black lines. C) Osr assays in wild type, *eri-1(mg366)* fed *R07G3.6* dsRNA, *osm-8(n1518)*, and *osm-8(n1518); exR07G3.6*. The percent of animals still motile after 10

minutes is indicated. N>40 animals for each genotype per timepoint. 'Ex' - extrachromosomal array. D) Osr phenotype of the indicated *osm-8* alleles and *osm-8* rescue constructs. All transgenes were generated in the *osm-8(n1518)* background and tested for rescue of the Osr phenotype. N>40 animals for each genotype. E) Rescue of the *osm-8*-induced *gpdh-1::GFP* expression phenotype by the R07G3.6 transgene. 'TG' = transgenic *osm-8;gpdh-1::GFP* animal carrying the R07G3.6; 'non-TG' = *osm-8;gpdh-1::GFP* only. Scale bar = 100 μ.
doi:10.1371/journal.pgen.1001267.g002

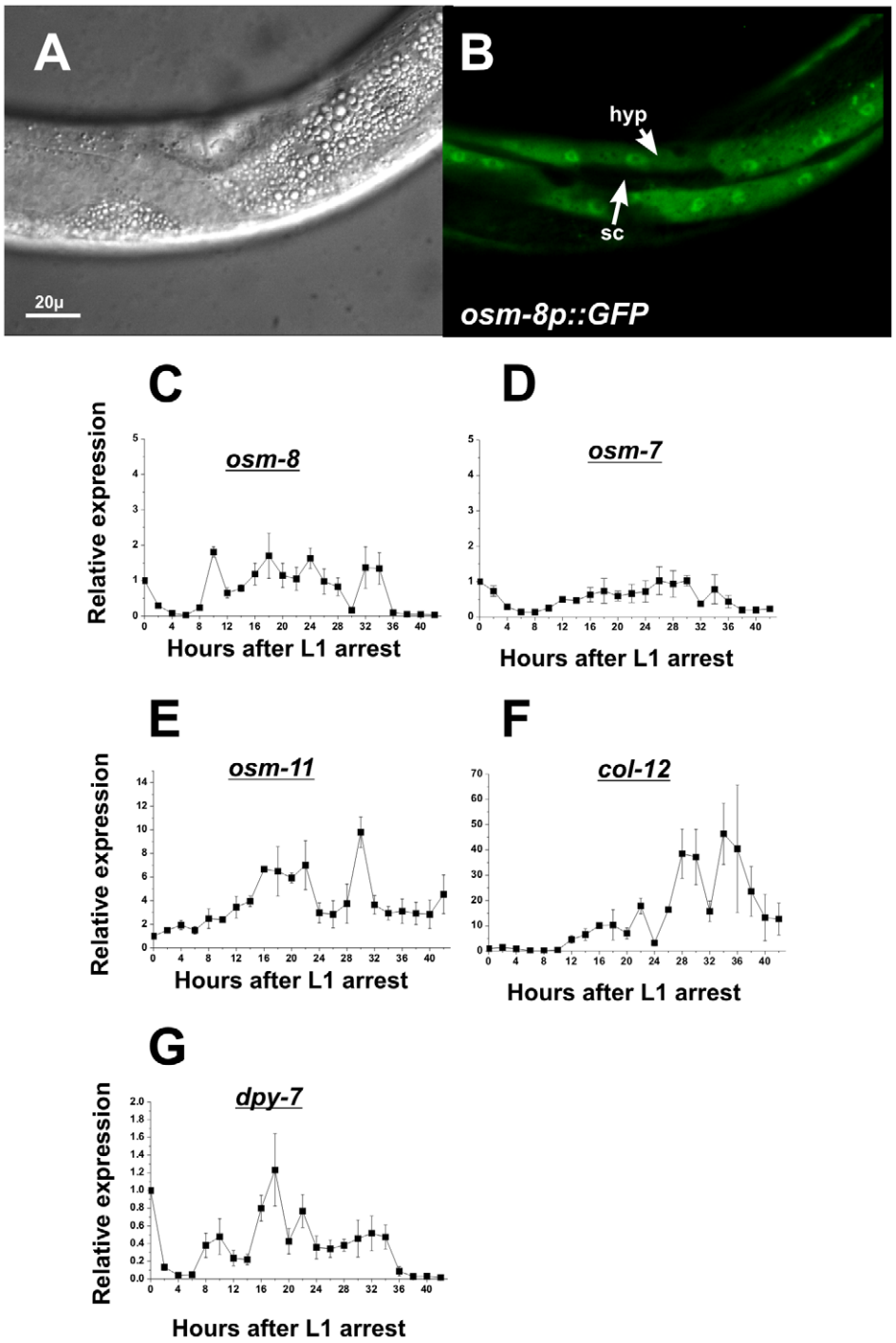


**Figure 3. *osm-8* is expressed in the hypodermis and is developmentally regulated.** A,B) DIC (A) and GFP (B) images of L4 stage animals expressing an *osm-8p::GFP* extrachromosomal array. 'hyp' - hypodermal syncitium; 'sc' - seam cell hypodermis. Scale bar = 20 μ. C-G) Quantitative PCR measurements of mRNA levels for the indicated gene through development. RNA isolations (N = 3) were performed as described in 'Materials and Methods' All mRNA levels were normalized to expression levels for actin (*act-2*), which did not change significantly throughout the timecourse (data not shown). All expression levels were normalized to data from T = 0 in order to generate relative gene expression levels.
doi:10.1371/journal.pgen.1001267.g003

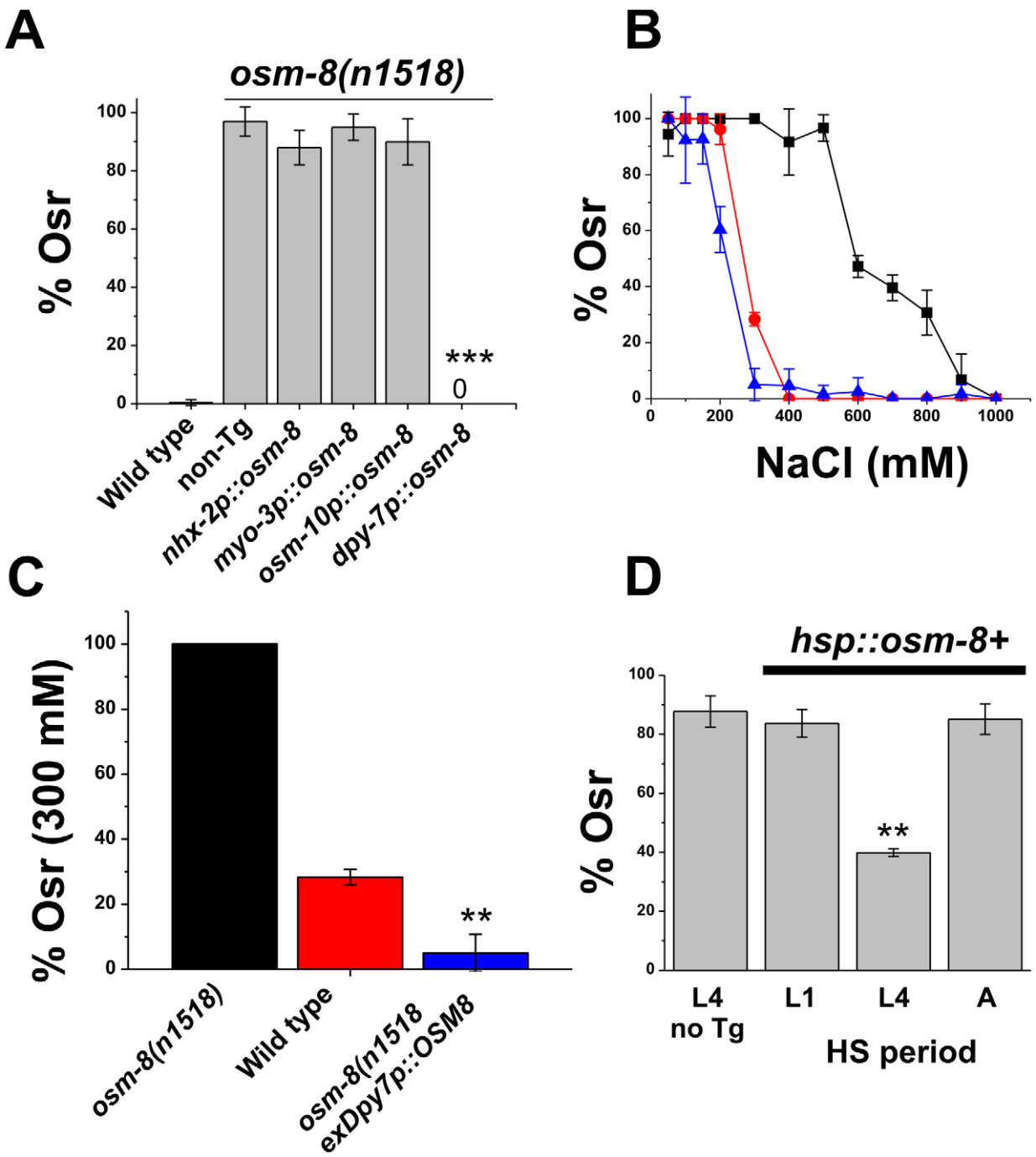


**Figure 4. Hypodermal expression of *osm-8* prior to extracellular matrix secretion is sufficient to rescue *osm-8* Osr mutant phenotypes.** A) Percentage of *osm-8* animals with an acute Osr phenotype following expression of *osm-8* from the indicated promoter. Data are the average from 3-5 independently derived lines for each construct. *nhx-2p* = intestine-specific; *myo-3p* = muscle specific; *osm-10p* = sensory neuron specific; *dpy-7p* = hypodermis specific. B) Dose-dependent acute Osr phenotypes of wild type (red circle), *osm-8(n1518)* (black square), and *osm-8(n1518);ex dpy-7p::OSM-8* (blue triangle) animals. N>40 animals per genotype for each concentration. C) Percentage of *osm-8(n1518)* animals with an acute Osr phenotype at 300 mM NaCl, from B. D) Percentage of *osm-8(n1518)* animals with an acute Osr phenotype following heat shock-induced expression of *osm-8*+ at the indicated time points. Heat shock induced expression of *osm-8* was confirmed by quantitative PCR (data not shown). 'L4 no Tg' indicates the negative control, which consisted of *osm-8(n1518)* animals lacking a transgene that underwent heat shock at the L4 stage. *** - $p<0.001$, ** - $p<0.01$.

doi:10.1371/journal.pgen.1001267.g004

regulator of osmosensitive signaling pathways, as a structural molecule that allows cells to detect osmotic alterations, or as a general regulator of cuticle organization and biosynthesis, disorganization of which might indirectly activate osmosensitive signaling pathways. To distinguish between these possibilities, we first used an inducible heat shock promoter to control the timing of expression of *osm-8* in an *osm-8(n1518)* background. Heat shock induction of *osm-8* in either the L1 or adult stage failed to rescue the

Osr phenotype in *osm-8* adult animals (Figure 4D). However, heat shock induced expression of *osm-8* in L4 animals exhibited significant rescue of the Osr phenotype of *osm-8* adults in multiple transgenic lines (Figure 4D). These data suggest that OSM-8 must be secreted from the apical membrane of the hypodermal cells between the L4 and adult stage in order to regulate adult osmosensitive responses. While these data suggest that OSM-8 is not required for early events in hypoderm development, they do not preclude the possibility that OSM-8 may be involved in late aspects of hypoderm development, such as seam cell fusion and cuticle synthesis.

Our expression studies and functional analyses suggested that OSM-8 is produced prior to or during the L4 molt. During this time, the adult cuticle is synthesized and secreted from the hypodermis [27]. Given that mutants affecting cuticle organization, such as *dpy-9* and *dpy-10*, phenocopy *osm-8* with regards to both the Osr phenotype and activation of osmosensitive gene expression [12,18,21], we considered the possibility that OSM-8 may also function as a structural component of the cuticle, like the DPY proteins, or as a general regulator of cuticle organization and/or biogenesis, even though *osm-8(n1518)* mutants do not exhibit a morphologically Dpy phenotype or have defects in cuticle permeability (Figure S3) or epidermal development (Figure S5). To test this hypothesis, we examined the localization of two cuticular markers, COL-19 and DPY-7, in *osm-8* mutant animals. *col-19* is expressed primarily during the L4-adult molt and the COL-19 protein marks the cuticular annuli [28]. *dpy-7* is expressed during all larval molts and DPY-7 protein is localized to the annular furrows [28]. In wild type young adult animals, both COL-19 and DPY-7 were localized in non-overlapping circumferential ring structures, as previously described [27] (Figure S6A, S6B, S6C) and this expression pattern was not significantly altered in *osm-8* mutants (Figure S6D, S6E, S6F). Furrow organization, as determined by measurements of the distance between adjacent DPY-7 stained furrows, was unaffected in *osm-8* mutants (Figure S6G). In contrast, *dpy-10* mutants, which disrupt collagen organization also have an Osr phenotype, lack furrows and do not exhibit any DPY-7 immunostaining staining [28] (and our unpublished observations). Together with our analysis AJM-1 localization in *osm-8* mutants (Figure S5), these data suggest that *osm-8* does not play a major structural or organizational role in the cuticle or in epidermal cell development and fusion, although more subtle alterations in cuticle or hypodermal organization that are not detectable at the level of the light microscope may be present. Moreover, since cuticle organization is disturbed in *dpy-9* and *dpy-10* mutants but not in *osm-8* mutants yet all of these mutants exhibit an Osr phenotype, our data suggest that cuticular disorganization is not the basis of the Osr phenotype.

## A genome-wide RNAi screen identifies *ptr-23* as a suppressor of *osm-8* phenotypes

Our data suggest that in *osm-8* mutants, the signaling pathways controlling osmotic stress responses are constitutively active. Inhibition of genes that function in such signaling pathways should block these pathways and suppress Osm-8 phenotypes. Previously, we demonstrated that two GATA transcription factors, *elt-2* and *elt-3*, function in the intestine and hypodermis, respectively, to promote osmotic stress resistance in both wild type and *osm-8* mutants [21]. To identify additional molecular components of these signaling pathways, we performed a genome-wide RNAi suppressor screen in the *osm-8; gpdh-1::GFP* background. Since *osm-8* mutants constitutively activate osmosensitive gene expression and are resistant to hyperosmotic stress (Figure 1), we screened for gene knockdowns that could suppress both the *gpdh-1::GFP* expression phenotype and the Osr phenotype of *osm-8* mutants (see 'Materials and Methods'). After screening ~18,000 RNAi clones (Figure 5), we identified 27 gene knockdowns that suppressed both phenotypes (Dataset S1). These 27 genes represented the intersection of 253 gene knockdowns that suppressed *osm-8*-dependent *gpdh-1p::GFP* overexpression (Dataset S2) and 84 gene knockdowns that suppressed the *osm-8*-dependent Osr phenotype (Dataset S3). The 27 *osm-8* suppressors did not alter motility under isotonic conditions and did not inhibit the expression of another stress inducible reporter in an activating genetic background (*upr-1(zc6); hsp-4p::GFP*) (Dataset S1). Functional classification of the *osm-8* suppressors revealed that many genes encode secreted, transmembrane, or extracellular matrix proteins, suggesting that the membrane-ECM interface plays a major role in controlling *osm-8* signaling pathways.

In yeast, the mucin-like proteins HKR1 and MSB2 function via the activity of a multipass transmembrane protein SHO1 to regulate osmotic stress resistance, osmosensitive gene expression, and glycerol accumulation [15]. Since SHO1 homologs are not present in *C. elegans*, we searched for candidate multi-pass transmembrane proteins among the list of *osm-8* suppressors that might encode candidate transducers of *osm-8* dependent extracellular signals. Within our list of 27 *osm-8* suppressors, we identified three non-mitochondrial multi-TM proteins - *vha-5*, *rhy-1*, and *ptr-23*. Previous studies have demonstrated that *vha-5* functions as a proton pump and regulates secretion [29] and that *rhy-1* is primarily localized to ER membranes [30]. Since the role of *ptr-23* was unknown, we chose to further characterize *ptr-23* function in the *osm-8* pathway. *ptr-23* (***P***a***t***ched-***r***elated protein 23) is distantly similar to the *Drosophila Patched* (Ptc) protein. In *Drosophila* and vertebrates, Ptc proteins are transmembrane receptors for the *Hedghog* (Hh) ligand. Hh signaling via Ptc proteins regulates developmental signaling events via the *Smoothened* (Smo) transmembrane protein and other downstream targets [31,32]. However, in *C. elegans*, sequence-based homologs of virtually all Hh signaling pathways components (*smoothened, fused, suppressor of fused, costal 2, costa*) are absent from the genome, suggesting that *C. elegans* does not express a canonical Hh signaling pathway [33]. Despite the absence of Hh signaling components, *C. elegans* contains many Patched and Patched-related genes, leading others to suggest that these transmembrane proteins have adopted novel Hh signaling-independent functions in *C. elegans* [34]. Both transcriptional and translational reporters revealed that *ptr-23* is co-expressed with *osm-8* in the hypodermis (Figure S7A, S7B, S7C, S7D). Furthermore, a PTR-23-GFP protein fusion, which is functional as measured by restoration of the Osr phenotype in an *osm-8(n1518); ptr-23(tm3762)* double mutant (Figure S7E) localizes to foci within specific areas of the hypodermis (Figure S7B). Functionally, *ptr-23(RNAi)* strongly suppressed *osm-8*-induced *gpdh-1::GFP* overexpression in both the intestine and hypodermis of adult animals (Figure 6A). The effect of *ptr-23(RNAi)* on *osm-8* regulated *gpdh-1* expression was specific, since *ptr-23(RNAi)* failed to suppress, and even significantly enhanced, the genetically induced expression of another stress-inducible reporter (*upr-1(zc6)*; *hsp-4::GFP* (Figure 6B). At a sequence homology level, *ptr-23* exhibits similarity to several other *ptr* genes, including *ptr-3*, *-8*, *-12*, and *-14*. However, *ptr-23(RNAi)* had no effect on the mRNA expression levels of these paralagous genes while it knocked down *ptr-23* mRNA levels by ~70%, suggesting that the observed phenotypes are not due to off-target effects of *ptr-23(RNAi)* treatment (Figure S8). Consistent with this, a *ptr-23* deletion allele, *tm3762*, fully suppressed the *gpdh-1p::GFP* overexpression phenotype of *osm-8(n1518)* mutants (Figure 8B). Together, these data show that loss of *ptr-23* specifically suppresses *osm-8* induced *gpdh-1* expression.

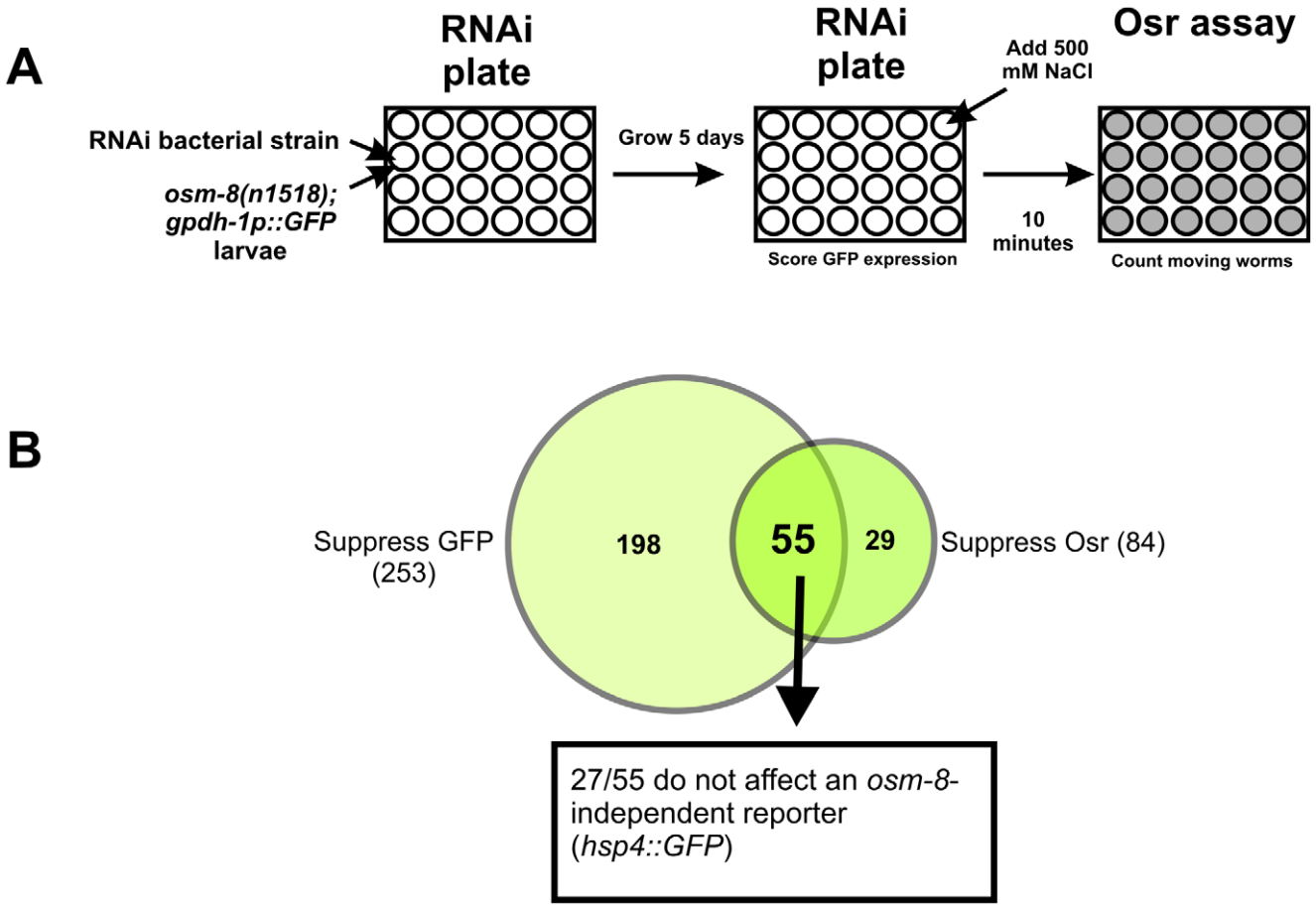


**Figure 5. A genome-wide RNAi screen identifies suppressors of *osm-8* phenotypes.** A) General strategy for the RNAi suppressor screen. B) Hits identified in the screen that suppress the *gpdh-1p::GFP* expression phenotype, the Osr phenotype, or both phenotypes. Overlap enrichment calculated using the normal approximation of the hypergeometric probability = 44.9 fold enrichment, p<4.333e-80 [47].
doi:10.1371/journal.pgen.1001267.g005

Previously, we demonstrated that hyperosmotic stress, as well as mutations in several *osr* genes (including *osm-8*), activate similar transcriptional programs [21]. To test whether *ptr-23* is generally required for *osm-8* regulated gene expression, we quantified the mRNA levels of several osmotically inducible genes in wild type, *osm-8*, and *osm-8; ptr-23* animals. Similar to its effects on *gpdh-1*, we found that *ptr-23(tm3762)* also eliminated the transcriptional upregulation of numerous genes induced by both hyperosmotic stress and *osm-8*, including *hmit-1.1*, *aqp-8*, *snf-3*, and several predicted antimicrobial genes *(cnc-3*, *-7*, and *nlp-28)* (Figure 6C). Interestingly, the expression of another group of predicted antimicrobial genes, including *nlp-29*, *nlp-31*, and *cnc-4*, did not decrease in the *osm-8; ptr-23* mutants, and were even found to be significantly increased. Therefore, *ptr-23* is required for the *osm-8*-dependent upregulation of many, but not all, osmotically induced genes, suggesting that *ptr-23*-dependent and *ptr-23*-independent pathways function downstream of *osm-8*.

Give that *ptr-23* suppresses most of the gene expression phenotypes of *osm-8*, we also wanted to determine if other Osm-8 phenotypes are suppressed by loss of *ptr-23*. We found that *ptr-23(tm3762)* fully suppressed the steady-state elevation of whole animal glycerol levels in *osm-8* mutants under isotonic conditions (Figure 7A). Furthermore, *ptr-23(tm3762)* mutants fully suppressed the Osr phenotype of *osm-8* mutants (Figure 7B). In addition to suppressing *osm-8*-mediated hyperosmotic stress resistance, *osm-8; ptr-23* double mutants demonstrated synergistic sensitivity to hypotonic stress (Figure S9), as neither single mutant exhibited this phenotype. Under hypo-osmotic conditions, we found that *osm-8; ptr-23* double mutants adopt a rigid rod-like phenotype and frequently explode within several minutes of exposure to the distilled water environment (Video S2, S3, S4, S5). This phenotype may be due to a general weakness of the cuticle brought on by the simultaneous loss of both *osm-8* and *ptr-23*. To test this hypothesis, we examined *bus-8* single mutants, which have weak and disorganized cuticles [23,24,25], and found that they also exhibit sensitivity to hypo-osmotic stress, although to a lesser extent than the *osm-8; ptr-23* double mutants (Figure S9). However, the sensitivity of *bus-8* mutants is partially suppressed in the *osm-8* background (Figure S9), demonstrating that such weakness, if it occurs, is not a general property of *osm-8* mutants but is rather due to a specific interaction between *osm-8* and *ptr-23*. Our data show that loss of *ptr-23* suppresses multiple Osm-8 phenotypes, including the overexpression of osmotically induced genes, glycerol accumulation, and osmotic stress resistance. Furthermore, *osm-8* and *ptr-23* exhibit a synergistic genetic interaction, as defined by the enhanced sensitivity of *osm-8; ptr-23* double mutants to hypo-osmotic stress.

While *ptr-23* mutations fully suppressed *osm-8(n1518)* phenotypes, we also examined whether *ptr-23* was required for wild type responses to hyperosmotic stress. We found that *ptr-23(tm3762)*

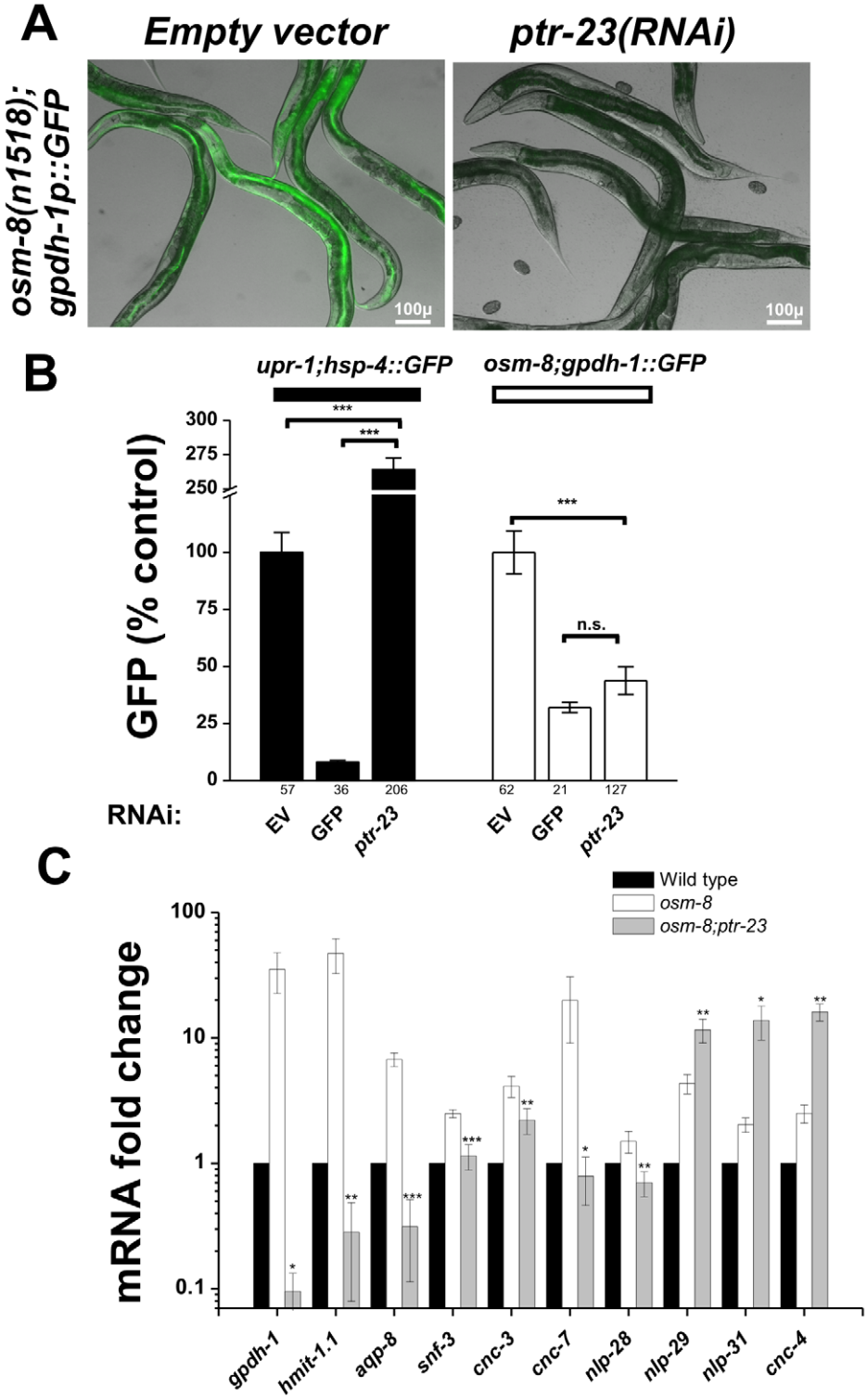


**Figure 6. *ptr-23* is required for *osm-8*–induced gene expression.** A) Fluorescence microscopy demonstrating suppression of *gpdh-1p::GFP* overexpression in the *osm-8(n1518)* background upon *ptr-23(RNAi)*. Identical results were obtained with the *ptr-23(tm3792)* deletion allele (see Figure 8). Scale bar = 100 µ. B) COPAS quantification of GFP expression from *upr-1;hsp-4::GFP* or *osm-8;gpdh-1p::GFP* animals fed empty vector (EV), GFP, or *ptr-23* dsRNA producing bacteria. The number of animals sorted for each condition is indicated below each bar graph. *** - $p<0.001$. C) qPCR quantification of the mRNA expression levels of the indicated osmotically inducible genes in wild type (black), *osm-8(n1518)* (white), and *osm-8(n1518); ptr-23(tm3762)* (gray) backgrounds. Expression levels are normalized to actin (*act-2*) and relative to wild type (set to 1) under isotonic conditions. N = 4 per genotype. * - $p<0.05$, ** - $p<0.01$, *** - $p<0.001$.
doi:10.1371/journal.pgen.1001267.g006

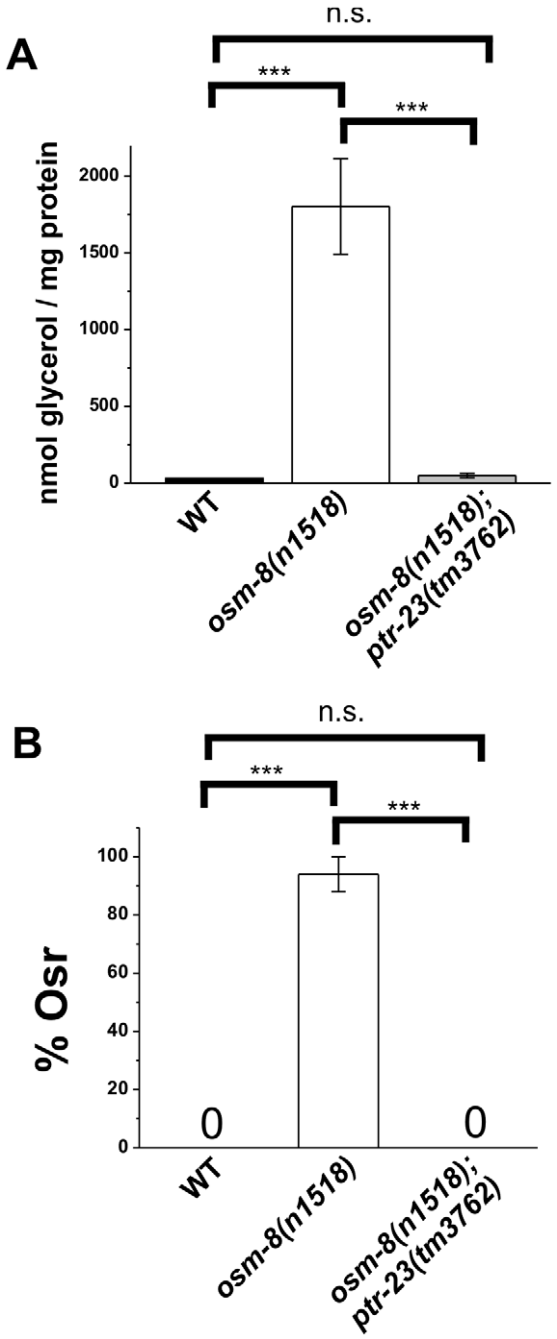


**Figure 7. *ptr-23* is required for *osm-8*–induced glycerol accumulation and Osr phenotypes.** A) Glycerol measurements from wild type (black), *osm-8*(n1518) (white), and *osm-8(n1518); ptr-23(tm3762)* (gray). N = 3–4 samples per genotype. *** - $p<0.001$, ** - $p<0.01$. B) Osr phenotype from wild type (black), *osm-8(n1518)* (white), and *osm-8(n1518); ptr-23(tm3762)* (gray). N>40 animals for each genotype.
doi:10.1371/journal.pgen.1001267.g007

mutants exhibited similar sensitivity to hyperosmotic stress as wild type animals (Figure 8A), suggesting that hyperosmotic stress resistance in *C. elegans* involves the activation of multiple redundant signaling pathways. Consistent with this hypothesis, *osm-8; ptr-23* mutants exhibit robust activation of *gpdh-1p::GFP* expression following exposure to 200 mM NaCl (Figure 8B). Together, our data suggest that *ptr-23* is required for signaling downstream of *osm-8* and that *ptr-23* signaling may be redundant with other osmosensitive signaling pathways that coordinate physiological responses to osmotic stress in *C. elegans*.

## Discussion

Using unbiased forward genetic approaches, we have molecularly identified the mucin-like protein OSM-8 as a key player in physiological responses to osmotic stress in *C. elegans*. We found that OSM-8 must be secreted from the apical membrane of the hypodermis prior to the L4 molt, suggesting that it acts in the cuticular space to carry out its function. A genome-wide RNAi suppressor screen identified the hypodermally expressed transmembrane protein PTR-23 as an essential and specific mediator of *osm-8* phenotypes, including activation of osmosensitive gene expression, glycerol accumulation, and Osr phenotypes. Together, our findings suggest an evolutionarily conserved role for mucin-like proteins in the transduction of osmotic stimuli and reveal unexpected functional redundancy in the *C. elegans* osmotic stress response.

The molecular mechanism(s) by which animal cells detect changes in osmolarity remains a major question in cell physiology. Our studies suggest that the mucin extracellular matrix, which is secreted by virtually all non-keratinized epithelial cells, may play a critical role in osmoregulatory physiology. Similar to previous *osr* genes [18,35], we found that the *osm-8* promoter is only expressed at detectable levels in the hypodermis and that the OSM-8 protein functions in the cuticular extracellular matrix to control osmoregulatory physiological process. Given its expression in epithelia, *osm-8* could contribute to osmoregulatory physiology in a number of direct or indirect ways, including the regulation of epithelial differentiation, cuticle permeability, cuticle structure, or direct regulation of osmosensitive signaling pathways. Our data argue against an indirect role for *osm-8* in this process, as *osm-8* animals have normally differentiated and fused hypoderm, normal cuticle permeability, and normal localization of major cuticle structural proteins. However, we note that during the time at which *osm-8* is required (L4 to adult transition), some additional developmental events occur, including the fusion of hypodermal seam cells and the synthesis and secretion of a new cuticle, both of which could be regulated by *osm-8*. While our data show that general cuticle markers and hypodermal cell fusions occur normally in *osm-8* mutants, we can not rule out the possibility that OSM-8 may be involved in these our other late developmental processes which are not assayed by the studies or markers presented here. Nonetheless, based on our data, we hypothesize that OSM-8 may function to directly regulate the signaling pathways controlling physiological responses to osmotic stress, such as osmosensitive gene expression and organic osmolyte accumulation. While our genetic experiments do not detail how such direct regulation might occur, the fact that *osm-8* must be expressed during the time of cuticle assembly and secretion but cannot function if supplied after this period suggests the possibility that OSM-8 may assemble into a static structural complex whose components exhibit little or no turnover. One intriguing and highly speculative possibility is that an OSM-8 protein complex in the cuticle directly detects changes in environmental osmolarity and transduces these signals through interacting proteins in the underlying hypodermal membrane. Such a complex could respond to changes in environmental osmolarity in a number of ways, including physical stretch/shrinkage, possibly via the OSM-8 mucin-like domain, the exposure or masking of signaling domains, or the acquisition/loss of protein interactions between the complex and underlying cell membrane. Clearly, further studies will be required to discriminate among these possibilities. Such studies may provide

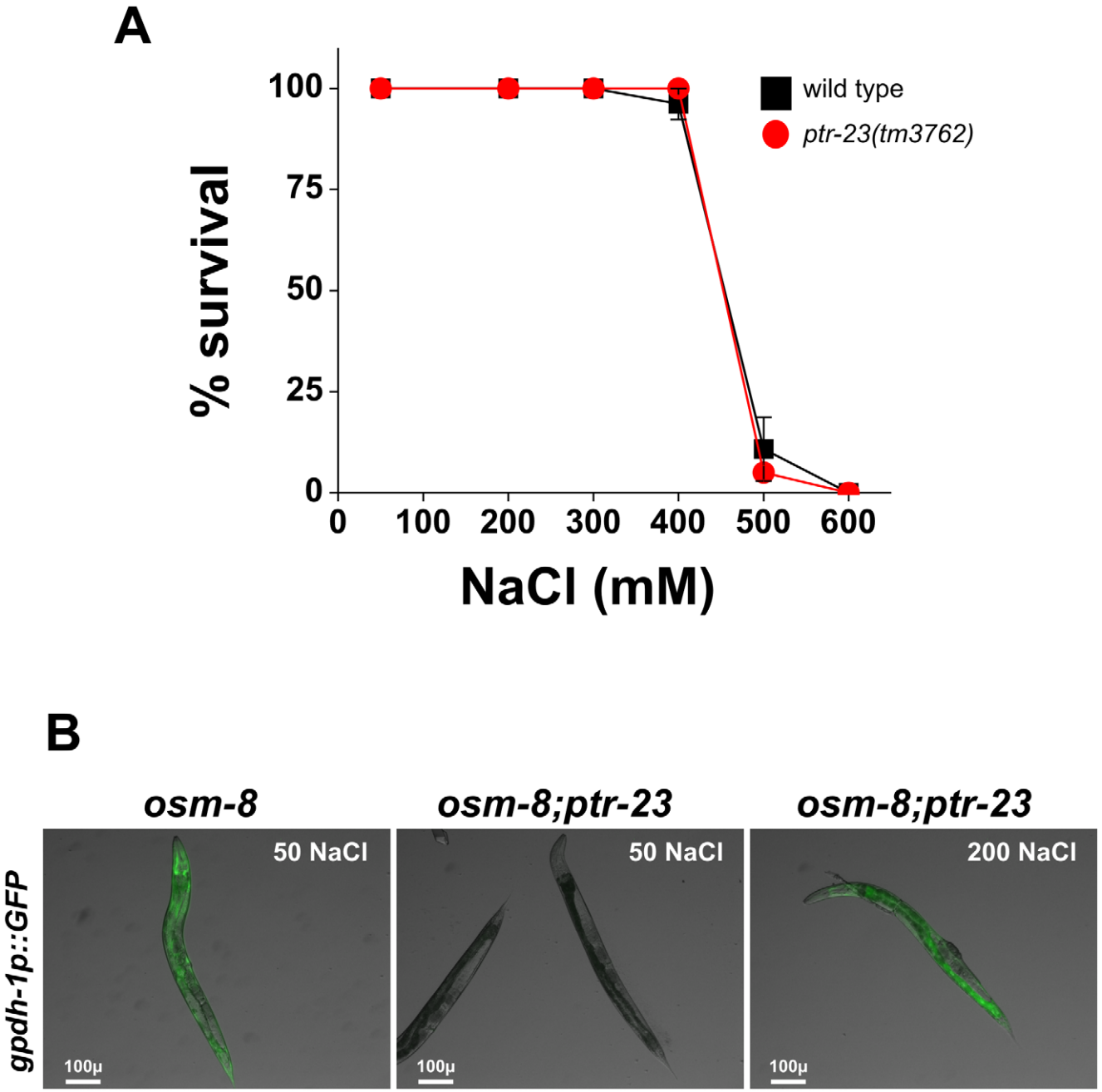


**Figure 8. *ptr-23* is not required for wild-type osmotic stress resistance or osmotic activation of *gpdh-1* expression.** A) Young adult wild type (black squares) or *ptr-23(tm3762)* (red circles) were exposed to the indicated levels of NaCl and the percentage surviving after 24 hours was determined. N>40 animals per genotype. B) Representative overlaid DIC and GFP images of young adult *osm-8(n1518)* (left) and *osm-8(n1518); ptr-23(tm3762)* (middle and right) carrying the *kbIs5(gpdh-1p::GFP; rol-6)* reporter. Animals were exposed to 50 mM NaCl or 200 mM NaCl for 18 hours as indicated.
doi:10.1371/journal.pgen.1001267.g008

new molecular and biophysical insights into the nature of osmosensing in *C. elegans* and other animals.

Interestingly, the general mechanism of mucin-dependent osmosensing described here is highly similar to that used by yeast, where the extracellular mucins Hkr1 and Msb2 transduce osmoregulatory signals through a plasma membrane-localized protein [15,36]. Although Hkr1 and Msb2 are both transmembrane mucins while OSM-8 is a secreted mucin, it was recently shown that the extracellular domain of Msb2 is proteolytically cleaved and that this non-membrane bound protein signals through the Sho1 transmembrane protein to control MAPK activation [37]. Therefore, non-membrane bound mucins can function as regulators of osmotic stress responses in both yeast and *C. elegans*. Remarkably, removal of the mucin domain from the yeast proteins results in a virtually identical phenotype to the phenotype caused by loss of *osm-8* in *C. elegans*, i.e. constitutive activation of osmosensitive gene expression. Based on our findings in *C. elegans* and these previous studies from yeast, we hypothesize that mucin-dependent signaling may also be an evolutionarily conserved mechanism of osmosensing in mammalian cells. Testing

this hypothesis in mammals will be challenging, as it will require analysis of cellular osmotic homeostasis mechanisms within native tissues, where complex mucin-dependent extracellular matrices can be assembled in the proper spatiotemporal manner. Given its optical transparency, simplified tissue and extracellular matrix organization, and well-described ultrastructure, *C. elegans* will continue to play an important role in understanding and testing how the extracellular matrix contributes to the highly conserved process of cellular osmoregulation.

While our data support a direct role for *osm-8* in the regulation of osmoregulatory physiology, other molecules must function downstream from OSM-8 to transduce osmosensitive signals. Using a genetic suppressor strategy, we identified the multi-pass transmembrane protein PTR-23 as being essential for multiple Osm-8 phenotypes. We also found that *osm-8* and *ptr-23* exhibit a synergistic interaction with respect to hypo-osmotic sensitivity. Both results strongly suggest that *osm-8* and *ptr-23* functionally interact with one another, although the nature of such interaction remains unknown. Such interactions could be direct, i.e. PTR-23 directly interacts with OSM-8 to transduce osmotic stimuli, or indirect, i.e. PTR-23 is required for the activity, synthesis, or localization of other molecules (proteins, lipids, metabolites, etc) required for transduction of *osm-8* signals. Further biochemical experiments will be needed to differentiate between these possibilities. Whatever the case, the signaling molecules/pathways that act to transduce *osm-8* initiated signals, either downstream of or in parallel to *ptr-23*, remain unknown. What might the molecular nature of such a pathway be? One possibility involves the p38 MAP kinase signaling pathway. Studies in yeast suggest that the mucins Msb2 and Hkr1, acting through Sho1, regulate the phosphorylation and activation of the p38 MAP kinase HOG1. If such regulatory mechanisms are conserved between yeast and *C. elegans*, one might predict that MAP kinases should be constitutively activated in *osm-8* mutants and that MAP kinase inhibition should suppress Osm-8 phenotypes. However, our screen did not identify any MAP kinases as suppressors of Osm-8 phenotypes (Dataset S1), although the significant false negative rate of RNAi screening in *C. elegans* means that such suppressors might have been missed. Furthermore, using phospho-specific p38 MAP kinase antibodies, we did not observe a significant increase in p38 MAP kinase phosphorylation in either *osm-8* or *osm-8; ptr-23(RNAi)* animals (data not shown). These findings are consistent with previous data demonstrating that deletion of the Hog1 homolog *pmk-1* has no effect on osmosensitive expression of antimicrobial genes [20] or *gpdh-1* (our unpublished data). Further genetic screening for *osm-8* suppressors, as well as directed testing of the numerous MAP kinase signaling homologs in *C. elegans* should help to reveal which MAP kinases, if any, direct osmoregulatory responses downstream of *osm-8* in *C. elegans*.

Interestingly, while loss of *ptr-23* can suppress Osm-8 phenotypes, it does not sensitize animals to hyperosmotic stress or block osmosensitive *gpdh-1* expression, suggesting the presence of a functionally redundant pathway(s) in the *C. elegans* osmotic stress response. Similar functional redundancy is also observed in the yeast osmoregulatory response, where loss of Sho1 does not block osmosensitive gene expression due to functional redundancy with the Sln1/Ssk2/Ssk22 pathway [38]. Our studies here suggest that similar functional redundancy is likely to occur in the *C. elegans* osmotic stress response, as defined both by the *ptr-23*-independent activation of *gpdh-1* expression by hyperosmotic stress and the continued upregulation of several antimicrobial peptides in *osm-8; ptr-23* animals. Although the molecular nature of these *ptr-23*-independent pathways is unclear, one possibility involves a pathway(s) that detects osmotically induced protein damage. We and others recently demonstrated that induction of protein damage is sufficient to activate osmosensitive gene expression and that genetic acceleration of protein damage sensitizes animals to hyperosmotic stress [3,12]. However, the molecular mechanisms for detecting such protein damage and activating osmoregulatory physiological responses, such as *gpdh-1* induction, have not yet been elucidated. Nonetheless, it seems unlikely that the protein damage sensing pathway represents the *ptr-23*-independent mechanism for regulating osmosensitive gene expression described in the present studies. Osmotically induced protein damage only occurs at extremely high (500 mM) extracellular NaCl concentrations over time periods of >1 h. In contrast, transcriptional activation of the osmosensitive gene *gpdh-1* is robust at significantly lower (200 mM) NaCl concentrations and occurs extremely rapidly (<15 minutes) [12,21]. Therefore, the response range and kinetics of osmotically induced protein damage is inconsistent with the range and kinetics of osmotically induced *gpdh-1* expression. This raises the possibility that multiple molecular mechanisms, functioning over discrete windows of osmolarity, may function in a complementary but separate manner to fine-tune osmoregulatory physiological responses. Further studies will be needed to determine the molecular details of these *ptr-23*-independent signaling pathways and their relationship to *osm-8* signaling.

We have shown that *osm-8*, a gene originally identified in a behavioral screen for avoidance of hyperosmotic stimuli, plays a central role in the regulation of whole animal osmoregulatory physiology and osmosensitive gene expression. Osmotic avoidance behavior is dependent on the ciliated sensory neuron ASH and its associated glial cells [39,40,41]. ASH interprets various sensory stimuli (mechanical, odors, osmotic) and initiates a behavioral avoidance response. Mutants that prevent osmotic detection by ASH were previously thought to affect two processes - cilia formation (i.e. *osm-3*/kinesin) and stimulus detection and/or signal amplification (i.e. *osm-9*/TRPV channel). Both of these processes function within the ASH cell. In contrast, *osm-8*, as well as other Osr genes which also exhibit osmotic avoidance behavior, are not expressed at detectable levels in ASH [18,19,35]. Instead, our data and previous findings demonstrate that these genes are expressed in the hypodermis and that mutations in these genes function to constitutively activate whole animal physiological responses normally induced in wild type animals by hyperosmotic conditions, such as upregulation of the glycerol biosynthetic enzyme *gpdh-1* in the intestine and hypodermis and glycerol accumulation. If *osr* genes are not expressed in ASH, then why does their loss cause defective osmotic avoidance behavior? One possible explanation is that changes in the physiological state of the animal, i.e. adaptation to hyperosmotic stress, may 'reset' the stimulus threshold of ASH to respond to a new stimulus level. If so, then other Osr mutants should also exhibit osmotic avoidance behavior. Indeed, the first identified Osr mutant, *osr-1*, exhibits defective osmotic avoidance behavior [19]. In the wild, this may allow *C. elegans* to exploit new environments that were previously aversive, provided that animals have adapted to such new conditions at the whole animal level. Given the abundance of genes that can mutate to an Osr phenotype [12,19], regulation of *osm-8* and the many other *osr* genes may play important roles in the evolution and adaptation of *C. elegans* within distinct environmental niches.

In conclusion, we have shown that the mucin-like protein OSM-8 plays a critical and specific role in osmoregulatory physiology in *C. elegans*. *osm-8* phenotypes are dependent on several proteins, including the transmembrane protein, PTR-23. Our findings reveal striking similarity in mechanism between *C. elegans* and yeast

osmosensing, with an extracellular mucin negatively regulating osmosensitive gene expression through the action of a transmembrane protein. We hypothesize that this general mechanistic strategy could be conserved from yeast to vertebrates and that mucin-regulated pathways may play important functional roles in mammalian osmoregulation.

## Materials and Methods

### *C. elegans* strains

All strains were maintained using standard culture methods and fed with the *E. coli* strain OP50. NGM media was made hypertonic by the addition of NaCl to the indicated concentration. The following strains were used: LGI: *ptr-23(tm3792)*, *kbIs5(gpdh-1p::GFP; rol-6);* LGII: *osm-8(n1518)*, *osm-8(ok3560*, *osm-8(tm3693); LGIII: osm-7(n1515); LGIV: eri-1(mg366); LGX: osm-11(n1604), bus-8(e2698)*, *wIs78* (*ajm-1::gfp; scm-1::gfp; unc-119(+); F58E10(+)*). Unless otherwise noted, all strains were grown at 20°C. Double mutants were created using standard genetic crossing methods and all genotypes were verified by PCR analysis and/or DNA sequencing. The wild type N2 strain was obtained from the *Caenorhabditis elegans* Genetic Stock Center.

### *osm-8* cloning

*osm-8(n1518)* was mapped between *dpy-2* and *vab-9* on LGII using standard multifactor mapping approaches. Consistent with this data, we found that the small deficiency *mcDf1*, which lies within the *dpy-2/vab-9* interval, failed to complement *n1518* mutants. Using a commercially available fosmid library (MRC GeneService, Cambridge), we purified overlapping fosmids spanning this interval and injected *osm-8(n1518); unc-119(ed3)* animals with pools of 3-5 fosmids (~25 ng/µl each), as well as an *unc-119*+ rescuing construct (150 ng/µl) [42]. Non-Unc transgenic animals were examined for rescue of the Osr phenotype. Identical rescue assays were carried out with purified fosmids or PCR products of R07G3.6.

### *C. elegans* transgenics and molecular biology

All transgenes were created using standard microinjection methods [43]. The *osm-8* rescue constructs were created using PCR fusion and sequenced to verify proper fusion [44]. The cell type specificity of each promoter was tested by replacing the *osm-8* coding sequence with that of GFP from the vector pPD95.75. In all cases, GFP expression was only observed in the predicted cell type. The *dpy-7p::osm-8* rescuing construct was injected at a concentration of 5 ng/µl, as our standard injection concentration (20–30 ng/µl) caused significant transgene-dependent lethality, suggesting that overexpression of *osm-8* is lethal. For the *hsp-16p::osm-8* construct, heat shock dependent induction was measured by qPCR and was determined to be >100-fold using a 1 hour 35° heat shock with recovery at 20°. For the *ptr-23p::PTR-23-GFP* construct, wild type or *osm-8(n1518); ptr-23(tm3762)* animals were injected at 30 ng/µl, along with a *myo3p::dsRed2* marker at 50 ng/µl. Primer sequences used for the generation of all expression constructs are listed in Dataset S4.

### RNA preparation and quantitative PCR

For the time course gene expression study in Figure 3, wild type animals were synchronized at 25°C as L1s using the hypochlorite method. L1 stage animals were seeded to NGM plates with OP50 and grown at 25°C. We chose to grow animals at 25°C to reduce the time window of the experiment and maintain synchrony within each individual experiment and between independent experiments as closely as possible. Animals were harvested for RNA isolation every two hours over 42 hours. The entire time course was replicated three times (i.e. RNA was harvested every two hours over 42 hours in three separate experiments). For other qPCR experiments (Figure 6, Figure S1, Figure S8), young adult animals grown at 20°C were used for RNA isolation. Animals were grown at 20°C for these experiments because *osm-8(n1518)* mutants grow poorly at 25°C. Purified total RNA was converted to cDNA (Superscript III, Invitrogen) and quantitative PCR was carried out on an ABI7300 qPCR system (Applied Biosystems) using the SYBR green method. Fold change was calculated using the auto CT function in SDS software (Applied Biosystems). Samples were normalized against expression levels for the actin gene *act-2*. Primer sequences for all of the probes used in this study are listed in Dataset S4. In most cases, primer pairs were designed to span across an intron, ensuring that amplification was biased to occur from cDNA and not genomic DNA. We also validated that each primer pair exhibited a copy number-dependent amplification relationship using a dilution series of wild type cDNA and verified the amplification of a single cDNA product by melting curve analysis and agarose gel electrophoresis.

### Osr and stress assays

Osr assays were carried out as previously described [18,19]. Animals were raised on standard NGM OP50 plates (50 mM NaCl) prior to the Osr assay. Oxidative stress assays were performed with synchronized young adults grown on NGM with OP50 (20°C). The animals where transferred into 300 µl of M9+200 mM paraquat (24 well plates, 6 animals per well) and scored at RT every 30 min For thermotolerance assays, NGM plates with OP50 were preheated to 35°C prior to placing young adult hermaphrodites onto the plates. Animals were scored as dead when they failed to respond to prodding with a platinum wire.

### COPAS analysis

Animals were washed from plates in M9 and placed directly into the sample cup of a COPAS Biosort (Union Biometrica). Gating parameters were established such that only L4 and older animals were analyzed. For each worm, the normalized green/TOF (Time-of-flight; measurement of worm length [45]) ratio was calculated and then divided by the mean green/TOF value of the control. For all COPAS assays, animals were measured in parallel on the same day.

### Microscopy and antibody staining

Synchronized young adults were fixed for immunostaining using a freeze fracture method. Following three washes with M9, worms were incubated on ice for 5 min and then washed with water. The worm pellet was resuspended in 80 µl of 0.025% gluteralaldehyde and frozen on dry ice between two SuperFrostPlus slides for at least 20 min. The slide sandwich was cracked open and the separated slides incubated in ice cold acetone for 5 min, followed by 5 min incubation in ice cold methanol. The slides were redhydrated through an EtOH wash (90%–50% ethanol, 5 min at −20°C) and the worms were collected in 1× PBS and stored at −30°C or used immediately for antibody staining. For antibody staining, the freeze fractured worms where incubated in blocking solution (1× PBS with 0.2% Gelatin, 0.25% Triton) for 30 min at RT and washed three times with PGT solutions (1× PBS with 0.1% Gelatin, 0.25% Triton). 200 µl PGT solution with the α-DPY7 antibody diluted 1:200 (kind gift of I. Johnstone, University of Glasgow) or pure PGT as a 'no primary antibody' control were added to a 30–50 µl pellet of worms and the probes incubated over night at 4°C with gently shaking. The primary antibody was

removed by washing the pellet 5× with washing solution (1× PBS with 0.25% Triton) and 200 µl of PGT solution containing an Alexa594 conjugated donkey anti-mouse secondary antibody (Invitrogen) was added to the pellet. After incubating for 3 h at room temperature, the worms were washed five times at room temperature and mounted onto slides in ProLong antifade (Molecular Probes). Z-stacked images were acquired on a Leica DMI4000 using a 1.42NA 63X lens and deconvolved in Leica AF6000 software.

### Genome-wide RNAi screen

RNAi screening was carried out as previously described [12]. Animals were screened using the MRC Geneservice feeding based RNAi library. We also screened a collection of RNAi clones targeting genes that were absent from the MRC library but present in the Open Biosystems ORFeome RNAi library. The estimated total number of genes targeted in the screen was 17,896. *osm-8(n1518); kbIs5 (gpdh-1p::GFP, rol-6(su1006))* animals were hypochlorite treatment and ~25 L1 animals were plated into wells of a 24 well plate seeded with 50 µl of RNAi bacteria. Worms were cultured at 16° until they reached the young adult stage (usually 96 hours). Animals were visually scored for GFP expression and motility using a fluorescence-equipped stereo dissecting microscope (Leica MZ16FA, Leica Microsystems). Immediately following visual scoring for GFP expression, 1 ml of 500 mM NaCl NGM solution was added to each well and the number of worms still moving after 10 minutes was determined. RNAi clones that suppressed either GFP expression or the Osr phenotype were rescreened in quadruplicate. During quadruplicate screening, wells were exposed to four different NaCl concentrations for Osr testing (50, 500, 700, 1000 mM) to determine the extent of Osr suppression. RNAi clones that suppressed the GFP expression phenotype as well as the Osr phenotype at 500 mM NaCl but had normal motility at 50 mM NaCl were considered strong suppressors. RNAi clones that suppressed the GFP expression phenotype as well as the Osr phenotype at 700 mM NaCl but not at 500 mM NaCl were consider weak suppressors and were not studied further. To confirm the specificity of the hits, RNAi clones were rescreened in the SJ6 strain (*upr-1(zc6); zcIs4 (hsp4p::GFP)*. SJ6 expresses an unfolded protein response reporter in the intestine in a genetically activated *upr-1* mutant background [46]. RNAi clones that suppressed GFP expression in *osm-8; gpdh-1p::GFP* but not SJ6 animals were considered to be specific suppressors of *osm-8*. The molecular identity of all final RNAi clones was confirmed by DNA sequencing. Gene knockdowns that suppressed the Osr phenotype (253 genes) or the *gpdh-1p::GFP* phenotype (84 genes) are listed in Dataset S2 and Dataset S3, respectively.

### Statistical analysis

Survival and gene expression data were analyzed using either the Student's T-test or one-way ANOVA, as implemented in Graphpad Prism (San Diego, CA) or Microsoft Excel. P-values $<0.05$ were taken to indicate significance.

## Supporting Information

**Dataset S1** RNAi gene knockdowns that suppress both osm-8 gpdh-1::GFP overexpression and Osr phenotypes.
Found at: doi:10.1371/journal.pgen.1001267.s001 (0.03 MB XLS)

**Dataset S2** RNAi gene knockdowns that suppress osm-8 gpdh-1::GFP overexpression phenotype.
Found at: doi:10.1371/journal.pgen.1001267.s002 (0.03 MB XLS)

**Dataset S3** RNAi gene knockdowns that suppress the osm-8 Osr phenotype.
Found at: doi:10.1371/journal.pgen.1001267.s003 (0.02 MB XLS)

**Dataset S4** Primers used in this study
Found at: doi:10.1371/journal.pgen.1001267.s004 (0.03 MB XLS)

**Figure S1** *osm-8(n1518)* mutants cause constitutive activation of transcriptional responses normally induced by hypertonic stress in wild type animals without activating the transcription of other stress-inducible genes. A) qPCR against the indicated genes was performed in young adult wild type animals exposed to 200 mM NaCl (black) or to *osm-8(n1518)* young adults exposed to 50 mM NaCl (white) as described in the 'Materials and Methods' section. Both conditions were normalized against the expression levels observed for wild type animals exposed to 50 mM NaCl. n = 3 for each condition/genotype. B) qPCR against the indicated heat shock proteins in wild type and *osm-8(n1518)* animals. N = 3 for each genotype.
Found at: doi:10.1371/journal.pgen.1001267.s005 (0.23 MB TIF)

**Figure S2** *osm-8(n1518)* mutants do not exhibit enhanced resistance to other stressors. A) Wild type (black) or *osm-8(n1518)* (red) young adults were exposed to oxidative stress (Paraquat, 200 mM in M9) and survival was measured every 30 minutes. N>30 animals for each genotype. B) Wild type (black) or *osm-8(n1518)* (red) young adults were exposed to heat shock (35° on pre-heated agar plates) and survival was scored every two hours. N>30 animals for each genotype
Found at: doi:10.1371/journal.pgen.1001267.s006 (0.20 MB TIF)

**Figure S3** *osm-8(n1518)* does not enhance or suppress cuticle permeability to Hoechst dye. Mixed-stage animals of the indicated genotypes were stained with the DNA dye Hoechst 33258 as a measure of cuticle permeability, as previously described [23,25] and hypodermal nuclei were imaged using fluorescence microscopy. '100 ms' and '1000 ms' refer to the camera exposure time. Scale bar = 20 µ.
Found at: doi:10.1371/journal.pgen.1001267.s007 (1.23 MB TIF)

**Figure S4** Enhancing the cuticle permeability of *osm-8(n1518)* mutants does not suppress the Osr phenotype. Animals of the indicated genotype were tested for the Osr phenotype. N>40 animals per genotype.
Found at: doi:10.1371/journal.pgen.1001267.s008 (0.19 MB TIF)

**Figure S5** *osm-8(n1518)* does not affect epidermal fusion events. *osm-8; wIs78* or *wIs78* animals, which express a functional AJM-1-GFP fusion protein as well as a seam cell nuclei GFP marker, were imaged at early (around L1 stage) and later (around L3-L4) stages of developments. Closed arrows point to the unfused (A,C) or fused (B,D) epidermal cell junctions. Open arrows point to the seam cell nuclei. Scale bar = 20 µ.
Found at: doi:10.1371/journal.pgen.1001267.s009 (1.02 MB TIF)

**Figure S6** *osm-8(n1518)* does not affect cuticle biogenesis or organization. Wide-field deconvolution microscopy of *col-19-GFP* fluorescence and α-DPY-7 antibody staining in young adult wild type (A-C) and *osm-8(n1518)* (D–F) animals. Scale bar – 10 µ. G) Mean distance between DPY-7 cuticular furrows in wild type (black) and *osm-8(n1518)* (white). n = 100 (*osm-8(n1518)* or 30 (N2) furrow measurements from at least 3 different animals.
Found at: doi:10.1371/journal.pgen.1001267.s010 (1.24 MB TIF)

**Figure S7** *ptr-23* is co-expressed with *osm-8* in the hypodermis. A & B) Young adult animal expressing a *ptr-23p::GFP* transcriptional

reporter. Scale bar = 250 μ. C & D) Young adult animal expressing a *ptr-23p::PTR-23-GFP* translational fusion reporter. This reporter rescued *ptr-23(tm3762)* phenotypes, suggesting it is functional. Scale bar = 20 μ. Arrows point to sites of PTR-23-GFP puncta. Similar expression patterns for both transcriptional and translational reporters were observed in 3 and 6 independently derived lines, respectively. E) Osr assay of *osm-8(n1518); ptr-23(tm3762)* animals that either do or do not carry the *ptr-23p::PTR-23-GFP* extrachromosomal array transgene. Data are averaged from three independently derived transgenic lines. N >15 for each genotype. * - $p<0.05$.
Found at: doi:10.1371/journal.pgen.1001267.s011 (0.60 MB TIF)

**Figure S8** *ptr-23(RNAi)* does not cause 'off-target' effects. qPCR of the mRNA expression levels or the indicated genes from wild type animals treated with either empty vector*(RNAi)* or *ptr-23(RNAi)*. A relative fold change of 1 indicates that the expression levels do not change following *ptr-23(RNAi)*. N = 3.
Found at: doi:10.1371/journal.pgen.1001267.s012 (0.16 MB TIF)

**Figure S9** *osm-8; ptr-23* animals exhibit synergistic sensitivity to hypo-osmotic stress. Young adult animals of the indicated genotypes were placed into distilled water and the percentage of animals not moving after ten minutes was quantified. N≥40 animals per genotype. *** - $p<0.001$, * - $p<0.05$.
Found at: doi:10.1371/journal.pgen.1001267.s013 (0.21 MB TIF)

**Video S1** Osr phenotype of *osm-8(n1518)* animals. Video recording of wild type or *osm-8(n1518)* young adult transferred from a standard NGM plate (51 mM NaCl) to liquid NGM containing 500 mM NaCl.
Found at: doi:10.1371/journal.pgen.1001267.s014 (1.44 MB WMV)

**Video S2** Exposure of wild type animals to distilled water. Video recording of wild type young adult animals fed empty vector RNAi bacteria that were transferred from a standard NGM plate to distilled water.
Found at: doi:10.1371/journal.pgen.1001267.s015 (2.06 MB WMV)

**Video S3** Exposure of *osm-8(n1518)* animals to distilled water. Video recording of *osm-8(n1518)* young adult animals fed empty vector RNAi bacteria that were transferred from a standard NGM plate to distilled water.
Found at: doi:10.1371/journal.pgen.1001267.s016 (2.08 MB WMV)

**Video S4** Exposure of *ptr-23(RNAi)* animals to distilled water. Video recording of wild type young adult animals fed *ptr-23(RNAi)* bacteria that were transferred from a standard NGM plate to distilled water.
Found at: doi:10.1371/journal.pgen.1001267.s017 (2.10 MB WMV)

**Video S5** Exposure of *osm-8(n1518); ptr-23(RNAi)* animals to distilled water. Video recording of *osm-8(n1518)* young adult animals fed *ptr-23(RNAi)* bacteria that were transferred from a standard NGM plate to distilled water.
Found at: doi:10.1371/journal.pgen.1001267.s018 (2.07 MB WMV)

## Acknowledgments

We thank Iain Johnstone for providing the *col-19-GFP* reporter strain and anti-DPY7 antibodies; Allison Frand for providing the *bus-8(e2698)* strain; members of the Lamitina, Sundaram, and Raizen labs for valuable discussions and reagents; and David Raizen and Meera Sundaram for providing helpful comments on the manuscript.

## Author Contributions

Conceived and designed the experiments: AKR TL. Performed the experiments: AKR YM LM LH TL. Analyzed the data: AKR YM LM LH TL. Contributed reagents/materials/analysis tools: TL. Wrote the paper: TL.

## References

1. Yancey PH, Clark ME, Hand SC, Bowlus RD, Somero GN (1982) Living with water stress: evolution of osmolyte systems. Science 217: 1214–1222.
2. O'Neill WC (1999) Physiological significance of volume-regulatory transporters. Am J Physiol 276: C995–C1011.
3. Choe KP, Strange K (2008) Genome-wide RNAi screen and in vivo protein aggregation reporters identify degradation of damaged proteins as an essential hypertonic stress response. Am J Physiol Cell Physiol 295: C1488–1498.
4. Burg MB (1995) Molecular basis of osmotic regulation. Am J Physiol 268: F983–996.
5. Burg MB (1994) Molecular basis for osmoregulation of organic osmolytes in renal medullary cells. J Exp Zool 268: 171–175.
6. Albertyn J, Hohmann S, Thevelein JM, Prior BA (1994) GPD1, which encodes glycerol-3-phosphate dehydrogenase, is essential for growth under osmotic stress in *Saccharomyces cerevisiae*, and its expression is regulated by the high-osmolarity glycerol response pathway. Mol Cell Biol 14: 4135–4144.
7. Smardo FL Jr., Burg MB, Garcia-Perez A (1992) Kidney aldose reductase gene transcription is osmotically regulated. Am J Physiol 262: C776–782.
8. Lamitina ST, Morrison R, Moeckel GW, Strange K (2004) Adaptation of the nematode *Caenorhabditis elegans* to extreme osmotic stress. Am J Physiol Cell Physiol 286: C785–791.
9. Yamauchi A, Nakanishi T, Takamitsu Y, Sugita M, Imai E, et al. (1994) In vivo osmoregulation of Na/myo-inositol cotransporter mRNA in rat kidney medulla. J Am Soc Nephrol 5: 62–67.
10. O'Rourke SM, Herskowitz I, O'Shea EK (2002) Yeast go the whole HOG for the hyperosmotic response. Trends Genet 18: 405–412.
11. Burg MB (2000) Macromolecular crowding as a cell volume sensor. Cell Physiol Biochem 10: 251–256.
12. Lamitina T, Huang CG, Strange K (2006) Genome-wide RNAi screening identifies protein damage as a regulator of osmoprotective gene expression. Proc Natl Acad Sci U S A 103: 12173–12178.
13. Thornton DJ, Rousseau K, McGuckin MA (2008) Structure and function of the polymeric mucins in airways mucus. Annu Rev Physiol 70: 459–486.
14. Tanaka T, Fillmore D, Sun S-T, Nishio I, Swislow G, et al. (1980) Phase Transitions in Ionic Gels. Phys Rev Letters 45: 1636–1639.
15. Tatebayashi K, Tanaka K, Yang HY, Yamamoto K, Matsushita Y, et al. (2007) Transmembrane mucins Hkr1 and Msb2 are putative osmosensors in the SHO1 branch of yeast HOG pathway. Embo J 26: 3521–3533.
16. de Nadal E, Real FX, Posas F (2007) Mucins, osmosensors in eukaryotic cells? Trends Cell Biol 17: 571–574.
17. Lamitina ST, Strange K (2005) Transcriptional targets of DAF-16 insulin signaling pathway protect *C. elegans* from extreme hypertonic stress. Am J Physiol Cell Physiol 288: C467–474.
18. Wheeler JM, Thomas JH (2006) Identification of a novel gene family involved in osmotic stress response in *Caenorhabditis elegans*. Genetics 174: 1327–1336.
19. Solomon A, Bandhakavi S, Jabbar S, Shah R, Beitel GJ, et al. (2004) *Caenorhabditis elegans* OSR-1 regulates behavioral and physiological responses to hyperosmotic environments. Genetics 167: 161–170.
20. Pujol N, Zugasti O, Wong D, Couillault C, Kurz CL, et al. (2008) Anti-fungal innate immunity in *C. elegans* is enhanced by evolutionary diversification of antimicrobial peptides. PLoS Pathog 4: e1000105. doi:10.1371/journal.ppat.1000105.
21. Rohlfing AK, Miteva Y, Hannenhalli S, Lamitina T (2010) Genetic and physiological activation of osmosensitive gene expression mimics transcriptional signatures of pathogen infection in *C. elegans*. PLoS ONE 5: e9010. doi:10.1371/journal.pone.0009010.
22. Culotti JG, Russell RL (1978) Osmotic avoidance defective mutants of the nematode *Caenorhabditis elegans*. Genetics 90: 243–256.
23. Partridge FA, Tearle AW, Gravato-Nobre MJ, Schafer WR, Hodgkin J (2008) The *C. elegans* glycosyltransferase BUS-8 has two distinct and essential roles in epidermal morphogenesis. Dev Biol 15;317(2): 549–59.
24. Gravato-Nobre MJ, Nicholas HR, Nijland R, O'Rourke D, Whittington DE, et al. (2005) Multiple genes affect sensitivity of *Caenorhabditis elegans* to the bacterial pathogen *Microbacterium nematophilum*. Genetics 171: 1033–1045.
25. Meli VS, Osuna B, Ruvkun G () Frand AR MLT-10 defines a family of DUF 644 and proline-rich repeat proteins involved in the molting cycle of *Caenorhabditis elegans*. Mol Biol Cell 21: 1648–1661.
26. Koh K, Rothman JH (2001) ELT-5 and ELT-6 are required continuously to regulate epidermal seam cell differentiation and cell fusion in *C. elegans*. Development 128: 2867–2880.

27. Page AP, Johnstone IL (2007) The cuticle. WormBook. pp 1–15.
28. McMahon L, Muriel JM, Roberts B, Quinn M, Johnstone IL (2003) Two sets of interacting collagens form functionally distinct substructures within a *Caenorhabditis elegans* extracellular matrix. Mol Biol Cell 14: 1366–1378.
29. Liegeois S, Benedetto A, Garnier JM, Schwab Y, Labouesse M (2006) The V0-ATPase mediates apical secretion of exosomes containing Hedgehog-related proteins in *Caenorhabditis elegans*. J Cell Biol 173: 949–961.
30. Shen C, Shao Z, Powell-Coffman JA (2006) The *Caenorhabditis elegans rhy-1* gene inhibits HIF-1 hypoxia-inducible factor activity in a negative feedback loop that does not include vhl-1. Genetics 174: 1205–1214.
31. Wetmore C (2003) Sonic hedgehog in normal and neoplastic proliferation: insight gained from human tumors and animal models. Curr Opin Genet Dev 13: 34–42.
32. Ingham PW, McMahon AP (2001) Hedgehog signaling in animal development: paradigms and principles. Genes Dev 15: 3059–3087.
33. Burglin TR, Kuwabara PE (2006) Homologs of the Hh signalling network in *C. elegans*. WormBook. pp 1–14.
34. Zugasti O, Rajan J, Kuwabara PE (2005) The function and expansion of the Patched- and Hedgehog-related homologs in *C. elegans*. Genome Res 15: 1402–1410.
35. Komatsu H, Chao MY, Larkins-Ford J, Corkins ME, Somers GA, et al. (2008) OSM-11 facilitates LIN-12 Notch signaling during *Caenorhabditis elegans* vulval development. PLoS Biol 6: e196. doi:10.1371/journal.pbio.0060196.
36. Pitoniak A, Birkaya B, Dionne HM, Vadaie N, Cullen PJ (2009) The signaling mucins Msb2 and Hkr1 differentially regulate the filamentation mitogen-activated protein kinase pathway and contribute to a multimodal response. Mol Biol Cell 20: 3101–3114.
37. Vadaie N, Dionne H, Akajagbor DS, Nickerson SR, Krysan DJ, et al. (2008) Cleavage of the signaling mucin Msb2 by the aspartyl protease Yps1 is required for MAPK activation in yeast. J Cell Biol 181: 1073–1081.
38. Tatebayashi K, Takekawa M, Saito H (2003) A docking site determining specificity of Pbs2 MAPKK for Ssk2/Ssk22 MAPKKKs in the yeast HOG pathway. Embo J 22: 3624–3634.
39. Maricq AV, Peckol E, Driscoll M, Bargmann CI (1995) Mechanosensory signalling in *C. elegans* mediated by the GLR-1 glutamate receptor. Nature 378: 78–81.
40. Hart AC, Sims S, Kaplan JM (1995) Synaptic code for sensory modalities revealed by *C. elegans* GLR-1 glutamate receptor. Nature 378: 82–85.
41. Bacaj T, Tevlin M, Lu Y, Shaham S (2008) Glia are essential for sensory organ function in *C. elegans*. Science 322: 744–747.
42. Maduro M, Pilgrim D (1995) Identification and cloning of *unc-119*, a gene expressed in the *Caenorhabditis elegans* nervous system. Genetics 141: 977–988.
43. Mello C, Fire A (1995) DNA transformation. Methods Cell Biol 48: 451–482.
44. Hobert O (2002) PCR fusion-based approach to create reporter gene constructs for expression analysis in transgenic *C. elegans*. Biotechniques 32: 728–730.
45. Pulak R (2006) Techniques for analysis, sorting, and dispensing of *C. elegans* on the COPAS flow-sorting system. Methods Mol Biol 351: 275–286.
46. Calfon M, Zeng H, Urano F, Till JH, Hubbard SR, et al. (2002) IRE1 couples endoplasmic reticulum load to secretory capacity by processing the XBP-1 mRNA. Nature 415: 92–96.
47. Kim SK, Lund J, Kiraly M, Duke K, Jiang M, et al. (2001) A gene expression map for *Caenorhabditis elegans*. Science 293: 2087–2092.